Article

Not peer-reviewed version

First U-pb (CA-ID-TIMS) Radioisotopic Dating of the Uppermost Permian Coal Interval in the Minusinsk Coal Basin (Siberia, Russia)

Vladimir V. Silantiev *, Sergey I. Arbuzov, Marion Tichomirowa, Alexandra Käßner, Alsu Kh. Izmailova, Sergey S. Ilenok, Bulat R. Soktoev, Nouria G. Nurgalieva, Yaroslav M. Gutak, Anastasia S. Felker, Lyubov G. Porokhovnichenko, Nikolai A. Eliseev, Veronika V. Zharinova, Evgenia M. Nurieva, Milyausha N. Urazaeva

Posted Date: 23 July 2024

doi: 10.20944/preprints202407.1814.v1

Keywords: Siberia, Minusinsk Basin; Permian; tonstein; ash falls, U-PB dating; CA-ID-TIMS, geochronology; biostratigraphy; Angaraland

Article

First U-Pb (CA-ID-TIMS) Radioisotopic Dating of the Uppermost Permian Coal Interval in the Minusinsk Coal Basin (Siberia, Russia)

Vladimir V. Silantiev *, Sergey I. Arbuzov, Marion Tichomirowa, Alexandra Käßner, Alsu Kh. Izmailova, Sergey S. Ilenok, Bulat R. Soktoev, Nouria G. Nurgalieva, Yaroslav M. Gutak, Anastasia S. Felker, Lyubov G. Porokhovnichenko, Nikolai A. Eliseev, Veronika V. Zharinova, Evgenia M. Nurieva and Milyausha N. Urazaeva

Affiliation: siarbuzov@mail.ru (S.I.A.); tichomir@mineral.tu-freiberg.de (M.T.); alexandra.kaessner@mineral.tu-freiberg.de (A.K.); alsu-izmaylova@mail.ru (A.K.I.); ilenokss@tpu.ru (S.S.I.); bulatsoktoev@tpu.ru (B.R.S.); nouria.nurgalieva@kpfu.ru (N.G.N.); gutakjaroslav@yandex.ru (Y.M.G.); lab@palaeoentomolog.ru (A.S.F.); plg@t-sk.ru (L.G.P.); yeliseev.21@mail.ru (N.A.E.); vevzharinova@kpfu.ru (V.V.Z.); evgeniya.nurieva@kpfu.ru (E.M.N.); milyausha.urazaeva@kpfu.ru (M.N.U.)
* Correspondence: vsilant@gmail.com

Abstract: This study presents the first U-Pb (CA-ID-TIMS) radioisotopic dating of zircon grains extracted from tonsteins (altered volcanic ashfalls) within the uppermost Permian coal interval of the Minusinsk Coal Basin (Siberia, Russia). Petrographic, structural, and mineralogical analyses confirm the volcanic ash origin of the tonsteins. The parent pyroclastic material is identified as rhyolite-pantellerite for tonstein I-22 and dacite-rhyodacite for tonstein I-12. Morphological analysis of zircon crystals, along with cathodoluminescence and melt inclusion studies, confirms their volcanic origin and crystallisation temperatures of 700–900ºC. New radioisotopic dates of 261.4 ± 0.7 Ma and 261.3 ± 0.4 Ma clarify the age of the Izykh Formation, enabling its direct correlation with the Capitanian Stage of the International Chronostratigraphic Chart. The results emphasise the possible discontinuity of the coal-bearing succession of southern Angaraland and highlight the potential for further stratigraphic refinement through continued radioisotopic dating of tonsteins.

Keywords: Siberia; Minusinsk Basin; Permian; tonstein; ash falls; U-PB dating; CA-ID-TIMS; geochronology; biostratigraphy; Angaraland

1. Introduction

Radioisotopic uranium-lead (U-Pb) dating of individual zircon grains by thermal ionisation mass spectrometry with isotope dilution and chemical abrasion (CA-ID-TIMS) is a widely accepted tool for the direct chronological correlation of local stratigraphic units with the International Chronostratigraphic Scheme (Schmitz et al., 2020; Wang et al., 2023). The application of U-Pb radioisotopic dating is particularly successful in coal-bearing sediments, which often contain numerous tonsteins, considered to be altered volcanic ashes originating from tectonic activity and explosive volcanism (Spears, 1970**;** 2012; Spears & Arbuzov, 2019; Lyons et al., 1994; Opluštil et al., 2022; Shen et al., 2021, 2023;).

Radioisotopic uranium-lead (U-Pb) dating has provided a chronostratigraphic framework for the coal basins of Euramerica (North America (Lyons et al., 2006), Western Europe (Ducassou et al., 2019; Jirásek et al., 2018; Opluštil et al., 2016, 2022; Pellenard et al., 2017), Eastern Europe (Donets Basin) (Davydov et al., 2010; 2012)); Gondwana (Australia (Metcalfe et al., 2015; Shi et al., 2022; Sobczak et al., 2024), South America (Cagliari et al., 2023; 2014; Guerra-Sommer et al., 2008; Jurigan et al., 2019; Mori et al., 2012; Simas et al., 2012)), and China (Feng et al., 2022; Wang et al., 2018; Zhang et al., 2023). In recent years, a number of radioisotopic ages from the Angaraland coal basins (Siberia) have been published, including data from the Irkutsk Basin (Mikheeva et al., 2020) and the Kuznetsk

 doi:10.20944/preprints202407.1814.v1

Basin (Davydov et al., 2021; Silantiev, et al., 2023; 2024). In this paper, we continue this series of publications and present the first radioisotopic age data for the Permian sediments of the Minusinsk Coal Basin.

The coal-bearing succession of the Minusinsk Coal Basin includes a large number of tonsteins, which have been studied very thoroughly from petrographic and geochemical viewpoints (Admakin, 1992; Arbuzov et al., 2003; 2017; Vergunov et al., 2019, 2020, 2024). Increased attention to the Minusinsk Coal Basin tonsteins is due to accumulations and elevated (up to industrially significant) Zr-Nb-Hf-Ta-REE-Ga contents confined either directly to them or to adjacent coal seams (Arbuzov et al., 2003; Vergunov et al., 2020, 2024). Many authors attribute high REE contents in coal seams to volcanic activity (Hower et al., 1999; Dai et al., 2010, 2017, 2018; Arbuzov et al., 2019).

The uppermost Permian coal-bearing interval, including two thick (up to 12 meters) coal seams, has been identified as the Izykh Formation (Fm) (Sivtchikov and Donova, 2016). Tonsteins containing zircon grains, dated by the radioisotopic method, were sampled from the XXX seam, located in the middle part of the formation.

As more collections were accumulated and more plant remains and invertebrate fossils were studied from the Izykh Fm, its biostratigraphic age became progressively younger. Initially, most researchers considered this stratigraphic interval to be early Permian, i.e., Asselian-Sakmarian (290–295 Ma) (Neiburg, 1938; Radchenko, 1955; Spasskaya, 1966; Gorelova, 1975; Dryagina, 1975; and others) and Artinskian-early Kungurian (280–290 Ma) (Troshkova and Zhichko, 1967). Later, the age of this interval began to be defined as the late Kungurian (about 275 Ma) (Betekhtina et al., 1988), and more recently as the Roadian (about 270 Ma) (Sivtchikov and Donova, 2016). The increased completeness of palaeobotanical collections and the involvement of microstructural investigations in the methodological approach to plant studies have resulted in a revision of the age of the Izykh Fm, from the Asselian-Sakmarian to the Roadian (Kazanian), making it approximately 20–25 Ma younger. This paper presents radioisotopic evidence that the Izykh Fm is approximately 10 million years younger than previously thought based on biostratigraphic data. This younger radioisotopic age aligns with biostratigraphic studies showing a trend towards a younger age for the Izykh Fm. However, the new radioisotopic data highlight the need to consider discontinuities in geological record, and the importance of further sampling and re-examining existing palaeontological collections using modern tools.

The aim of this paper is to present the first data on the radioisotopic age of the Permian coal-bearing strata of the Minusinsk Basin, which enables direct correlation with the International Chronostratigraphic Chart. The objectives of the work included: 1) fieldwork involving the search and sampling of tonsteins; 2) petrographic and geochemical study of tonsteins; 3) extraction of zircon grains from tonsteins; 4) confirmation of the volcanogenic nature of zircon grains; 5) radioisotopic dating using the CA-ID-TIMS method and analysis of radioisotopic data; 6) comparison of radioisotopic age with biostratigraphic data.

2. Geological Background

The Minusinsk Coal Basin is one of the Late Palaeozoic coal basins of the Altai-Sayan Fold Belt (Figure 1A,B) and is situated in the south part of the Minusinsk intermountain trough, a complex synclinorium extending submeridionally for almost 300 km along the Yenisei and Chulym River valleys. The Minusinsk intermountain trough borders with the pre-Devonian fold structures of the Kuznetsk Alatau (to the west), the Western Sayan (to the south and southeast), and the Eastern Sayan (to the east), and in the north it is joined with the West Siberian Plate (Fedotova and Fedotov, 2002; Arbuzov et al., 2003).

 doi:10.20944/preprints202407.1814.v1

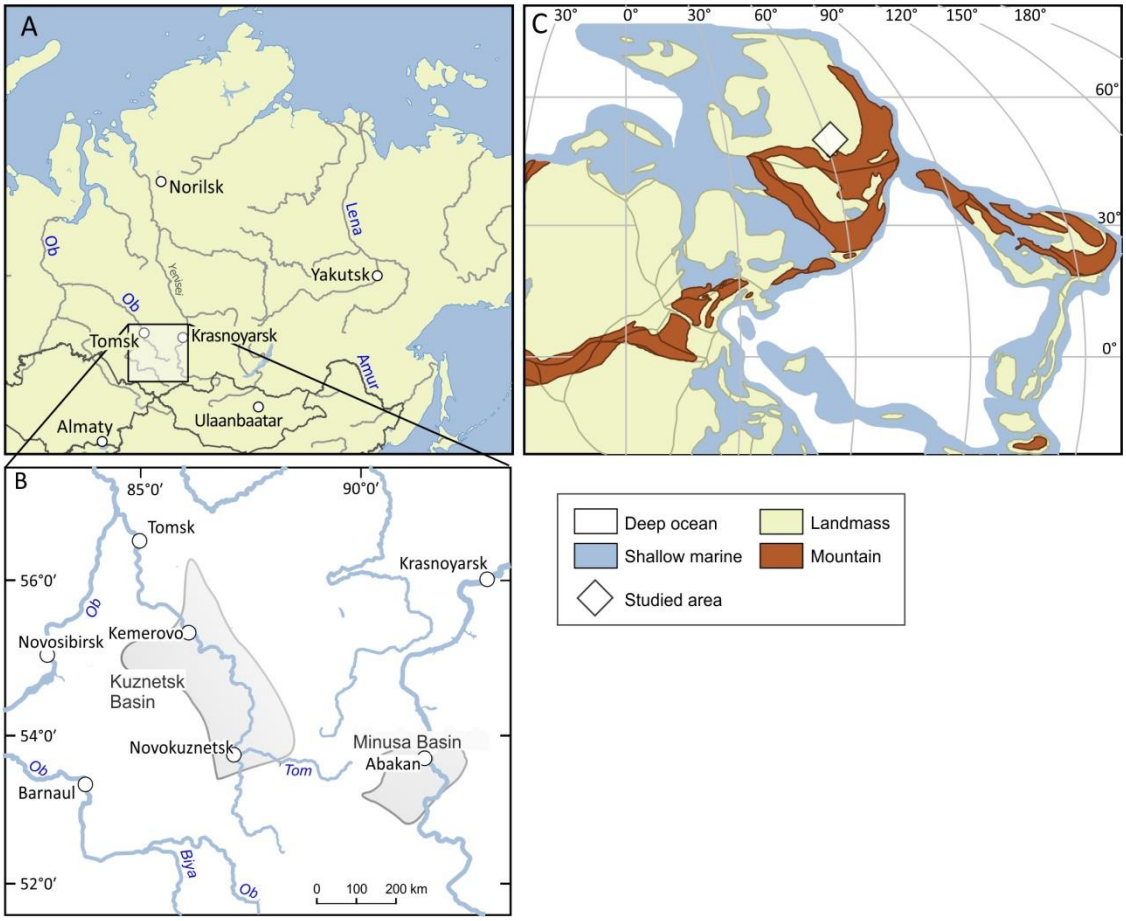

Figure 1. Location of the studied area: (A) overview map, (B) location scheme of the Kuznetsk and Minusinsk Coal Basins; (C) position of the studied area on the Late Permian palaeogeographic map compiled using the free software QGIS and Gplates, and the datasets provided by (Cao et al., 2017).

The Minusinsk intermountain trough includes a number of subordinate local Late Palaeozoic depressions and uplifts that are superposed on the Caledonian fold basement. The basement of the trough was formed in the late Cambrian-early Devonian and is represented by various metamorphic rocks of the Precambrian and lower Palaeozoic, along with intrusions of different age and composition. The basement is situated at a depth of 6000–7000 m and is exposed at the surface in the surrounding fold structures of the Kuznetsk Alatau, the Eastern and Western Sayan. The sedimentary cover comprises volcaniclastic, clastic and coal-bearing sediments of the Middle Devonian (Givetian), Carboniferous and Permian, as well as Mesozoic and Cenozoic deposits.

The lower boundary of the coal-bearing limnic succession is unconformable and is accepted at the base of a thin conglomerate overlain by coal-bearing shales and coals, dated as Serpukhovian by plant and invertebrate fossils. It is assumed that most of the coal-bearing sediments of the Minusinsk intermountain trough have been destroyed by post-Mesozoic erosion (Fedotova and Fedotov, 2002), and the remaining part (1100 to 1800 m thick) is preserved mainly in the south of the trough in several synclines (or muldes) which are referred to as the Minusinsk Coal Basin. The total area of the Minusinsk Coal Basin is 8,100 km^2, while the area of commercial coal measures is about 1,100 km^2. The coal-bearing succession includes sediments from the late Early Carboniferous to the late Middle Permian (Figure 2).

The first stratigraphic scheme of the coal-bearing succession of the Minusinsk Coal Basin and a 1:200,000 scale geological map were developed in the late 1920s. Subsequently, the stratigraphic schemes and geological maps were detailed in the 1940s–1970s. In 1997, Victor Sivtchikov (Sivtchikov and Donova, 2016) revised the stratigraphic scheme of the coal-bearing succession based on new paleontological data and a comprehensive summary of all available materials. This revised scheme is currently used for the latest geological maps (Fedotov et al., 2019), and we adopt it in this paper.

Preprints.org (www.preprints.org) | NOT PEER-REVIEWED | Posted: 23 July 2024 doi:10.20944/preprints202407.1814.v1

The Minusinsk Coal Basin is subdivided into several synclines (or *muldes*), which are separated from each other by anticlinal folds (Figure 3). The territory we studied is part of the Izykh Mulde, representing a rounded isometric structure with a flat bottom and sloping (10–15 to 30°) sides (Figure 4). The diameter of the mulde along the basement of the Serpukhovian coal-bearing sediments is 25 km. The mulde is composed of coal-bearing sediments accumulated from the late Early Carboniferous (Mississippian, Serpukhovian) to the late Middle Permian (Guadalupian, Capitanian).

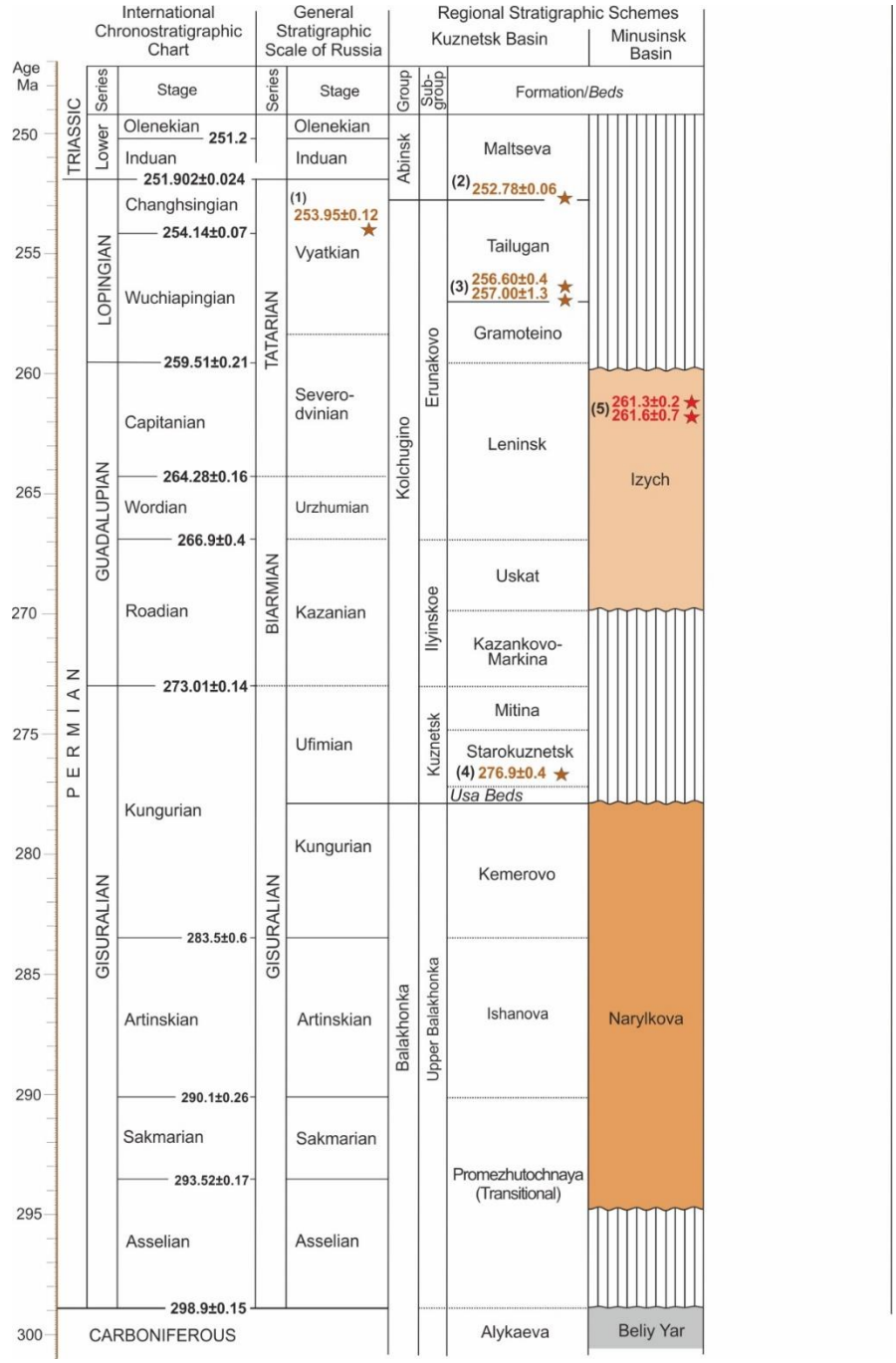

Figure 2. Regional Stratigraphic Scheme of the Permian of the Minusinsk Coal Basin (Fedotov et al., 2019), with modifications based on new radioisotopic datings; its correlation with the Regional Scheme of the Kuznetsk Basin (Decisions…, 1982; Budnikov, 1996) and comparison with the General Stratigraphic Scale of Russia (Stratigraphic Guide…, 2019) and the International Chronostratigraphic Chart (International…, 2023). Radioisotopic datings highlighted with star symbols are based on (1) ref. (Davydov et al., 2020); (2) ref. (Davydov et al., 2021); (3) ref. (Silantiev et al., 2023); (4) ref. (Silantiev et al., 2024); (5) this article.

Preprints.org (www.preprints.org) | NOT PEER-REVIEWED | Posted: 23 July 2024 doi:10.20944/preprints202407.1814.v1

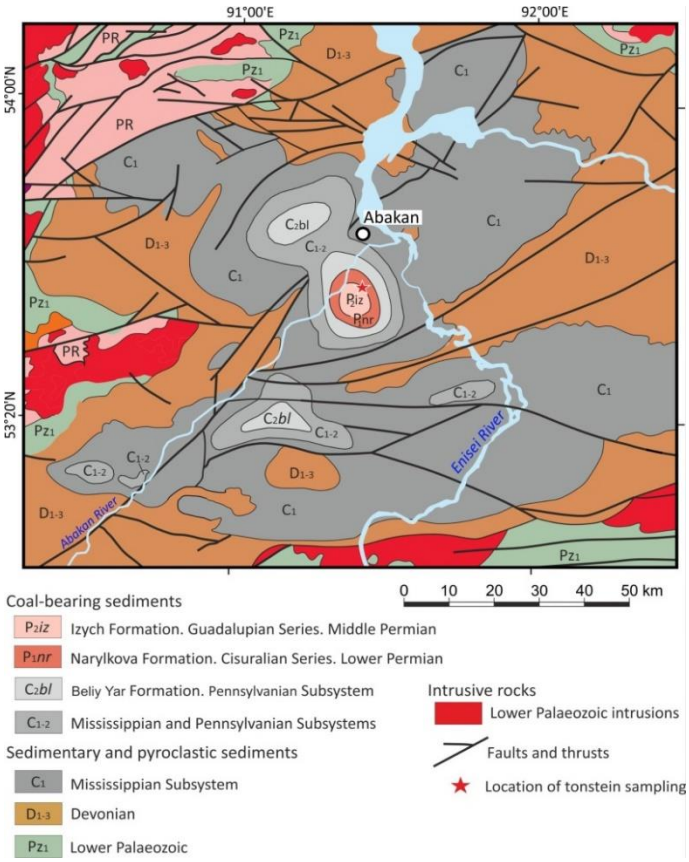

Figure 3. Geological map of the Minusinsk Coal Basin (simplified from (Bezzubtsev and Perfilova, 2008)) and sampling location within the Izykh syncline (mulde).

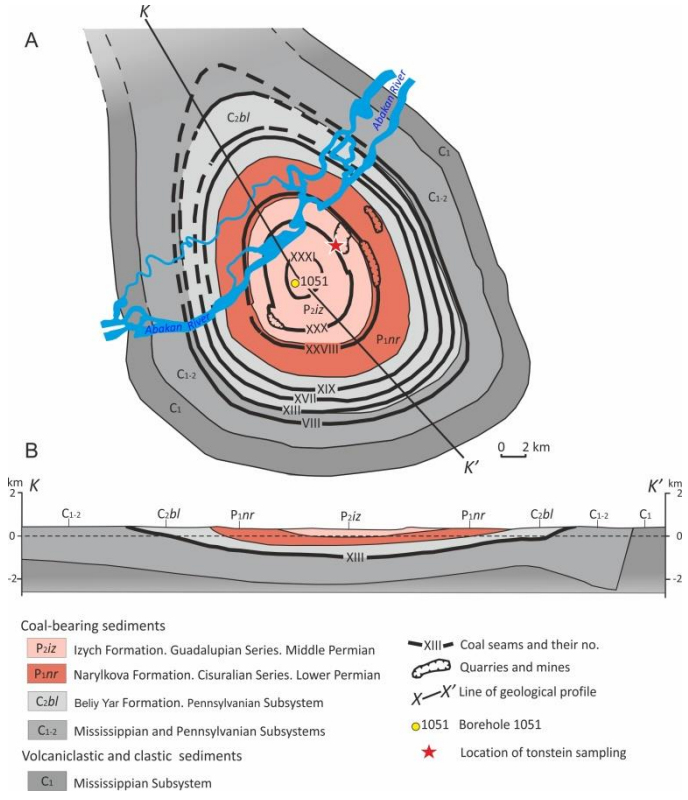

Figure 4. Geological map of the Izykh syncline (mulde) (A) and profile on line X–X′ (B) (simplified from (Fedotova and Fedotov, 2002)); sampling location is highlighted with star symbol.

 doi:10.20944/preprints202407.1814.v1

Coal-bearing sediments are composed predominantly of siltstones (50%), sandstones (30%), mudstones (10%) and coals (6%); other rocks such as conglomerates, gravelites, limestones are of subordinate importance.

The productive coal deposits of the Minusinsk Basin include 122 coal seams and interbeds, of which 35 are contiguous or split coal seams. Generally, the main coal seams preserved from erosion are traceable in all the basin muldes.

Each syncline (or mulde) of the basin is considered a separate coalfield, with its own index system for coal seams. In particular, the coal seams of the Izykh Mulde are numbered with Roman numerals from I to XXXI. Additional coal seams above the main seam are indexed by the number of the main seam with a letter in upper case (e.g., XV^{a}, XV^{b}, etc.). Additional coal seams below the main seam are marked by the main seam number with one or several apostrophes (e.g., XV', XV'', etc.).

The *Izykh Fm* (P2iz), which is the subject of this article, is distributed only in the central part of the Izykh Mulde (see Figures 3 and 4). It is agreed that the lower boundary of the Fm coincides with the top of coal seam XXVIII. The Izykh Fm (P2iz) includes coal seams XXIX to XXXI and overlies the Narylkova Fm with an unconformity (Figure 5). The duration of this unconformity is estimated to span from the late Kungurian to the early Roadian (Figure 2).

The *Izykh* Fm (P2iz) (250–260 m) is composed predominantly of siltstones (more than 50%), including coal seams, interlayers of shales and sandstones, and subordinate lenses of siderites and conglomerates. The rocks include an admixture of ash material. At 30–35 m above the base of the formation, a surface of erosion and unconformity is established. *The lower part* of the Izykh Fm (140–150 m) is represented by a coal-free interval consisting of siltstones and sandstones with only one thin coal seam (XXIX) and several local interlayers. Up the section, the number and thickness of sandstone beds increase. *The upper part* of the formation (100–110 m) is composed primarily of fine-grained clastic rocks, including siltstones, shales, and fine sandstones. It also features two thick coal seams, indexed as XXX and XXXI.

The XXX coal seam (in total 4.0–9.3 m) typically comprises 5–7 coal beds with a thickness of 0.1 to 6.5 m, separated by rock interlayers with a thickness ranging from 0.3 to 3.0 metres. In certain locations, the XXX seam is divided into additional seams, designated as XXXa and XXXb. The coals of the XXX seam are characterised by heterogeneity of composition, caused by the interbedding of semi-glossy, matte, and semi-matte coals. The vitrinite reflectance varies between 0.58% and 0.62%, which corresponds to the first stage of coal metamorphism (Fedotova and Fedotov, 2002). The XXX seam contains a number of tonsteins (from 1 to 30 cm thick) which were sampled for zircons (see the Material section). The geochemical characteristics of these tonsteins were previously studied in detail by a number of the authors of this paper (Vergunov et al., 2020; 2024).

Tonsteins. A notable feature of the coal seams in the Minusinsk Basin is the widespread distribution of thin beds of altered volcanic ash, commonly referred to as tonsteins. The thickness of such beds usually varies from several millimetres to 5 cm (Admakin, 1992). In coal seams, tonsteins typically form packs comprising several beds arranged at a distance of 5 to 30 cm from each other. The intervals between adjacent packs are several metres.

Clastic intervals intercalated with coal seams sometimes also contain single tonsteins which are confined to thin clayey rocks. Tonsteins can be confidently traced over long distances and are often used for correlation purposes. The primary ash material of tonsteins is altered to kaolinite.

Preprints.org (www.preprints.org) | NOT PEER-REVIEWED | Posted: 23 July 2024 doi:10.20944/preprints202407.1814.v1

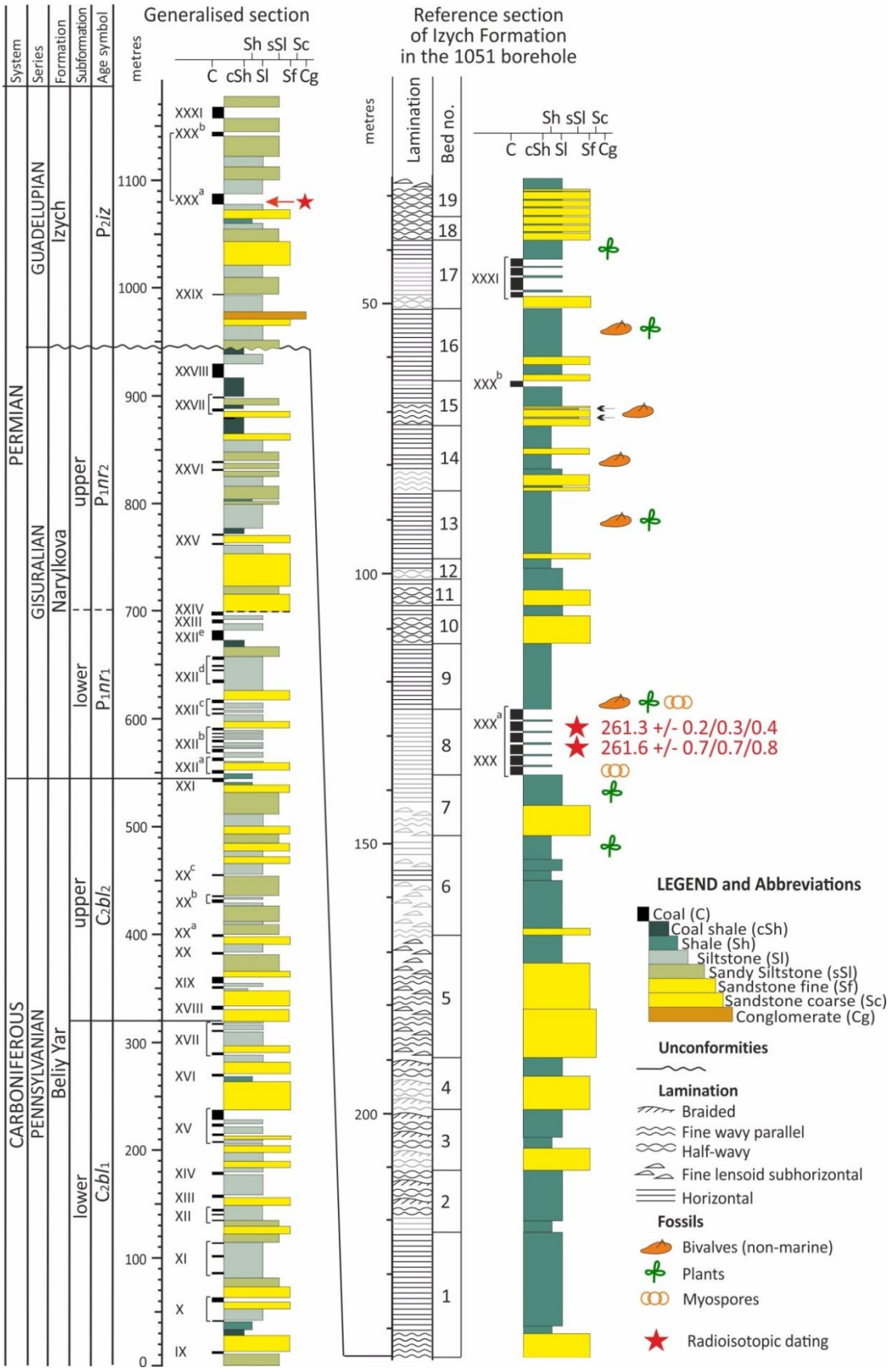

Figure 5. Generalised stratigraphic section of the Upper Carboniferous (Pennsylvanian) and Permian (Cisuralian and Guadalupian) of the Minusinsk Coal Basin (compiled from (Fedotova and Fedotov, 2002; Arbuzov et al., 2003; Fedotov et al., 2019)) (A) and Reference section of Izych Formation in the 1051 borehole, Izych coalfield (compiled by V. M. Yadrenkin in (Sivtchikov and Donova, 2016)); the star symbols indicate the radioisotopic dating discussed in this article.

 doi:10.20944/preprints202407.1814.v1

According to Admakin (1992), the coal seams of the Minusinsk Basin comprise two distinct types of tonsteins: granular and cryptocrystalline. In addition to authigenic kaolinite, the composition of tonsteins may include quartz, sanidine, zircon, apatite, and other minerals. Kaolinite is often represented by pseudomorphoses of plagioclase and microcline. Zircon crystals display pleochroic halos of brown kaolinite, which exhibit a darker colouration due to either a change in the charge of the chromophore atom or defects in the crystal structure resulting from radioactive emission. It has been assumed that the composition of the primary tuffs varies from andesite to pantellerite. The most plausible hypothesis for the accumulation of this material is periodic ashfalls, which formed successive series (packs) of beds (Arbuzov et al., 2003).

3. Materials

Samples of tonsteins for zircon extraction were taken in 2015 and 2018 within the Izykh open-cast coal mine from the XXX and XXX^{a} seams, which lie just above the middle of the Izykh Fm (Figures 4–6). In the coal seams, tonsteins appear as light-coloured thin continuous layers of siltstone or mudstone traceable for kilometres. Two tonsteins, 1–2 cm thick, were collected from each coal seam (see Figure 7). The fifth tonstein sample was collected from a siltstone parting (0.45 m thick) with increased radioactivity (25 μR/h) separating coal seams XXX and XXX^{a}. The tonstein I-12 from seam XXX^{a} and the tonstein I-22 from the siltstone parting were the only samples that contained zircon grains in sufficient quantity for radioisotopic dating. In total, approximately 200 zircon grains were extracted from the two tonsteins and analysed using a range of methods.

Figure 6. Outcrop of the upper part of the Izykh Fm in the Izykh coal mine showing the location of tonstein sampling.

Preprints.org (www.preprints.org) | NOT PEER-REVIEWED | Posted: 23 July 2024 doi:10.20944/preprints202407.1814.v1

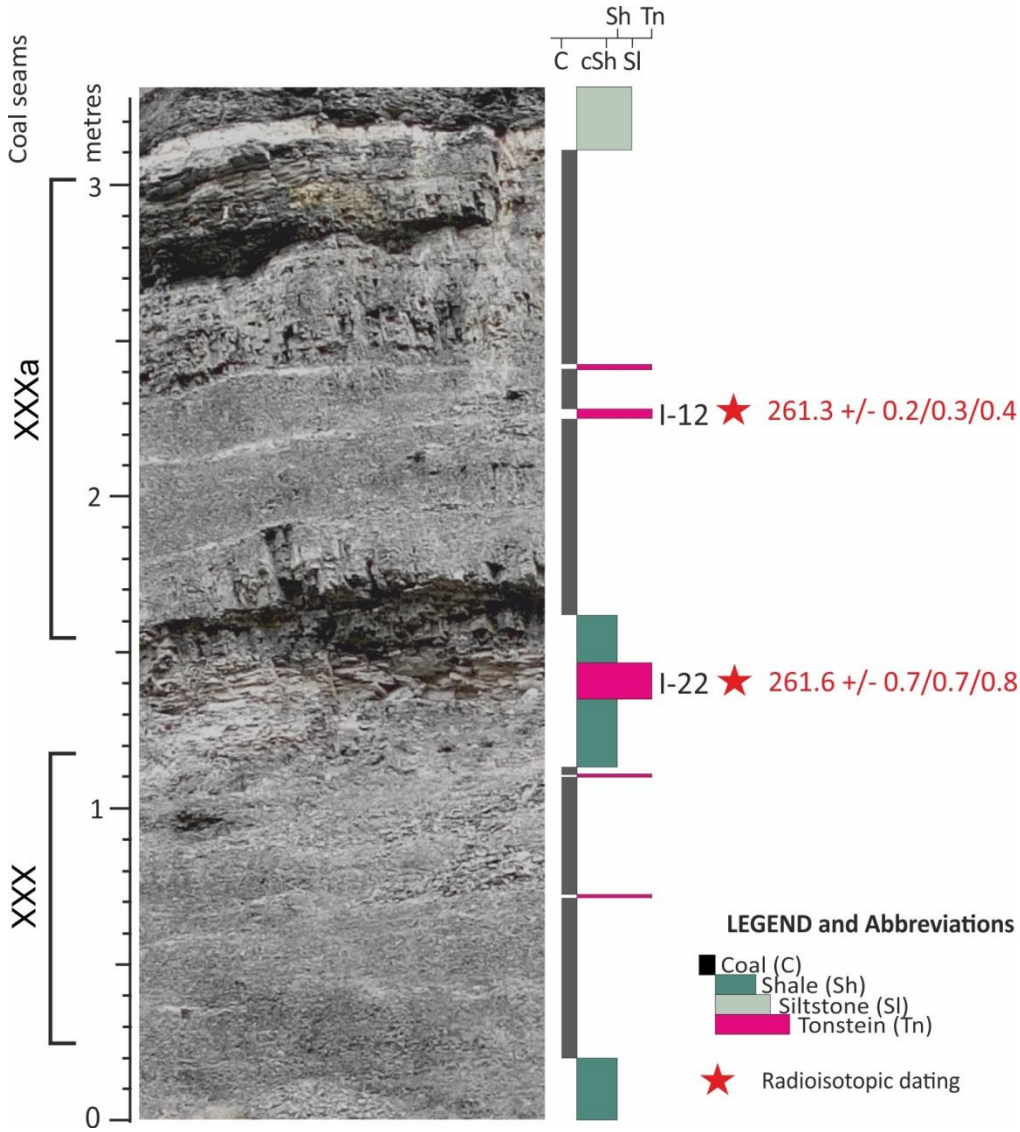

Figure 7. Location of tonsteins I-12 and I-22 in coal seams XXXa and XXX.

Tonsteins are soft (though not fragile) clayey rocks that range in colour from light yellowish-grey to greyish-brown (Figure 8). When wet, they take on a darker hue. Some samples display secondary subhorizontal cleavage, similar to lamination. They feel like dry soap when touched.

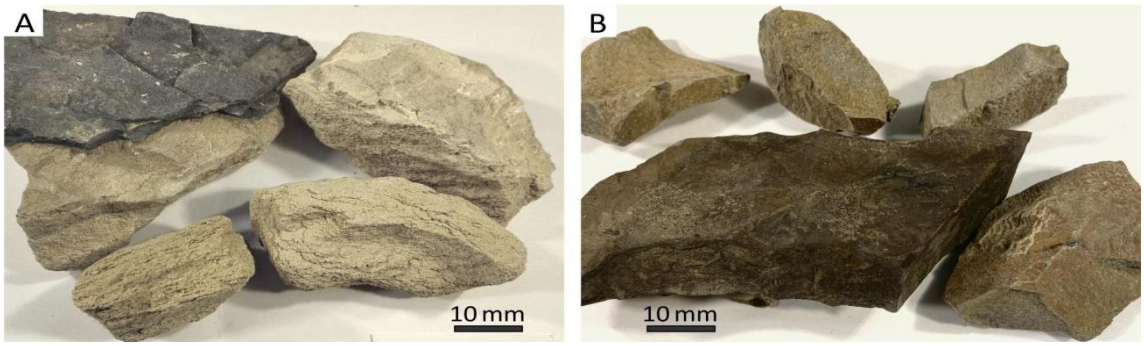

Figure 8. Tonstein samples from the coal seams XXXa and XXX: (a) tonstein I-12; the upper left sample retained contact with the adjacent coal and (b) tonstein I-22; the darker sample is wet.

 doi:10.20944/preprints202407.1814.v1

The zircons extracted from tonsteins I-12 and I-22 show no visible features of transportation or roundness (Figure 9). They appear as monomineral associations, indicating that they were not subjected to any significant external influences during their accumulation in tonstein.

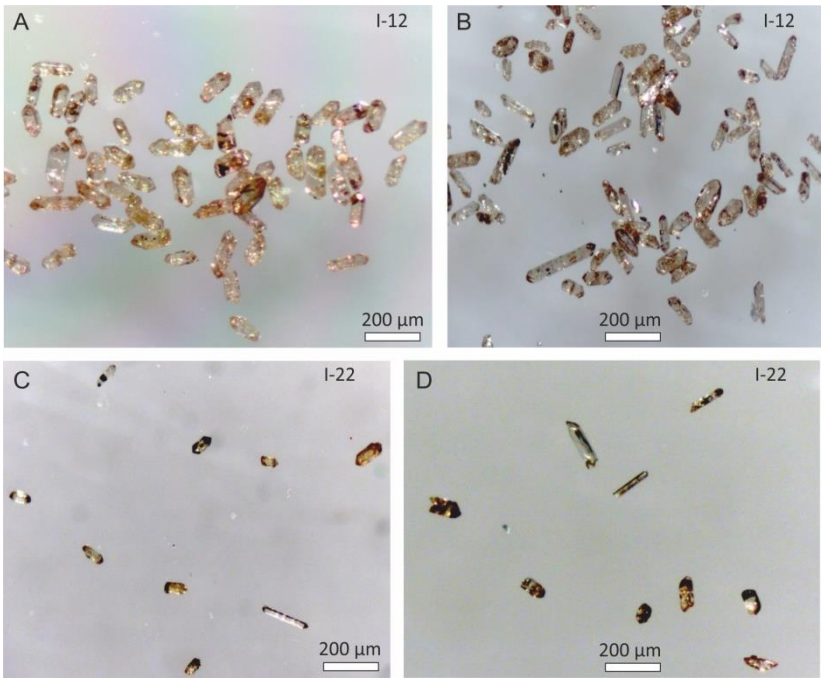

Figure 9. Zircon grains extracted from tonsteins I-12 (A, B) and I-22 (C, D) .

4. Methods

In this study, we apply a number of traditional and modern methods for detailed study of tonsteins and zircons extracted from them. The main objective of all these methods is to confirm the volcanogenic origin of the zircon grains used for radioisotopic dating. A brief description of the methods is given below.

X-ray diffraction analysis was conducted in the Laboratory of Lithology of the Tomsk Scientific Research and Design Institute of Oil and Gas using the RIGAKU ULTIMA IV X-ray diffractometer (Japan) with the integration of X-ray film imaging in Brega-Brentano geometry (performed by B.R. Soktoev). The following parameters were used for the diffraction patterns: Cu anode, X-ray tube voltage of 40 kV, current of 30 mA, power of 1.2 kW, imaging speed of 1°/min, pitch of 0.02°, and imaging angles of 2Θ from 5° to 70°. To improve the quality of XRD and facilitate the identification of low-content minerals, specific sample processing techniques were employed (Moore and Reynolds, 1997). A Rietveld analysis was conducted using PDXL and Siroquant software (Taylor 1991) to perform quantitative mineralogical calculations on the whole rock data (Bish and Post 1993).

Electron microscopy and X-ray energy-dispersive spectrometry of tonsteins was performed at the International Innovative Scientific and Educational Centre "Uranium Geology" of the Engineering School of Natural Resources of the National Research Tomsk Polytechnic University on a Hitachi S-3400N scanning electron microscope (Japan) equipped with a Bruker X@Flash 5010 X-ray energy-dispersive spectrometer (Germany). The study of samples was carried out in low vacuum mode, using backscattered electrons.

Inductively coupled plasma mass spectrometry (ICP-MS) was employed to analyse the elemental composition of tonsteins using the iCAP Qc equipment (ThermoFisher Scientific, Germany) at the Institute of Geology and Petroleum Technologies of Kazan Federal University. The standard sample preparation process was carried out using the Ethos Up microwave decomposition oven (Milestone, Italy). The prepared solution was analysed on a mass spectrometer that had been calibrated with multi-element standards at concentrations ranging from 1 to 100 ppb for each

 doi:10.20944/preprints202407.1814.v1

element. The resulting values were then recalculated to the initial concentration, taking into account the blank sample, suspension and dilution of the solution.

Analysis of the Morphological Features of Zircon Crystals. The aim of the study was to verify the volcanogenic origin of zircon crystals (zirconium orthosilicate, $Zr(SiO_4)$) extracted from tonsteins. As is widely recognized, zircon crystallises in a tetragonal syngony. Additionally, zirconium is frequently isomorphically substituted by uranium, thorium, and other radioactive elements. The zirconium crystal lattice is highly susceptible to changes in the chemical composition of the growth medium and the crystallisation temperature. Variations in these parameters result in the crystallisation of different morphotypes, including short prismatic, isometric and needle-like crystals (Markl, 2008).

The morphology of zircon crystals was studied in accordance with the approach proposed by J. Pupin (1980), utilising the diagram he devised (Figure 10), which correlates the shape of crystals with the crystallisation temperature. The study of morphology focused on three key areas: a) habitus, which determines the dominant simple crystallographic form; b) the perfection of the crystal facets or the degree of idiomorphism; c) the character of facets, including the presence of combinational hatching, deformation, abrasion, signs of dissolution and secondary recrystallisation.

Scanning electron microscope images of zircon grains (over 150) were obtained at the Institute of Geology of the Technical University of Freiberg Mining Academy using a JEOL JSM-7001F Field Emission Scanning Electron Microscope (Japan).

Cathodoluminescence was applied to study the internal structure of zircon crystals and to select homogeneous crystals for radioisotopic dating. Heterogeneous zircons characterised by the presence of ancient cores and young facets were not used for dating. Sample preparation of zircon grains for cathodoluminescence was carried out using epoxy resin, abrasives (10, 5 and 1 micron) and Struers RotoPol 35 grinding equipment (Germany). Cathodoluminescence photography (more than 150 images) was carried out at the Institute of Geology of the Technical University of Freiberg Mining Academy on a JEOL JSM- 7001F microscope.

The study of gas-liquid (fluid) inclusions in zircon grains (5 grains from each tonstein sample) was carried out at Kazan Federal University, Institute of Geology and Oil and Gas Technologies, using Linkam THMS600 (United Kingdom) with the operating temperature range from –196°C to 600°C.

 doi:10.20944/preprints202407.1814.v1

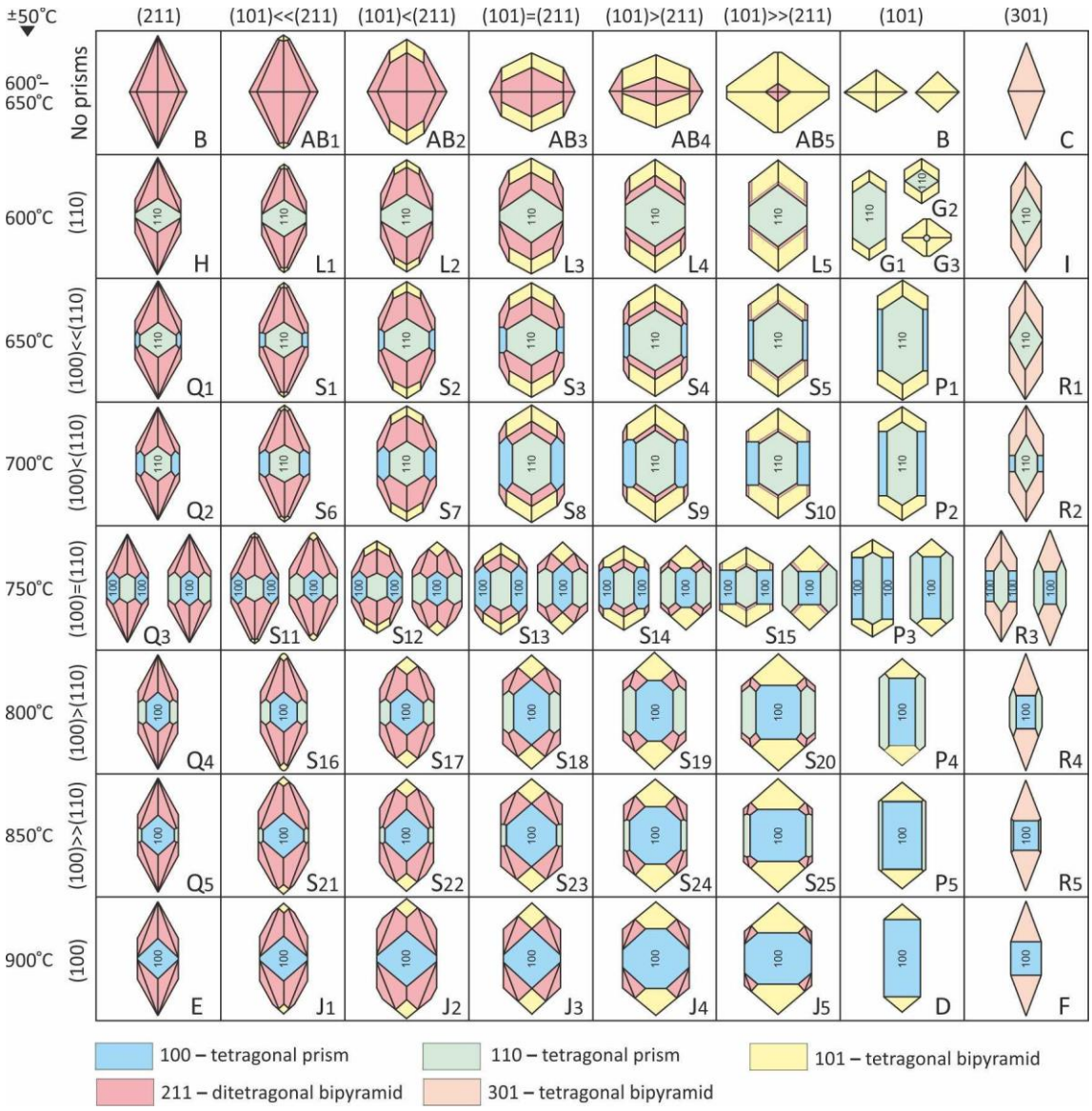

Figure 10. Main types and subtypes of zircon crystals and the corresponding geothermometric scale according to J.P. Pupin (1980). The letter designations of crystal types and subtypes are provided in accordance with the classification system of J.P. Pupin (1980, p. 209, Table 1).

Radioisotopic dating methods. Tonstein samples were processed at the Kazan Federal University. The most promising zircon grains were then sent to the Isotopic Laboratory, Institute of Mineralogy, Technische Universität Bergakademie Freiberg (Germany), for precise dating using CA-ID-TIMS.

Zircon extraction. Zircons were extracted from the tonsteins using three standard procedures involving dimethyl sulfoxide ($(CH_3)_2SO$), ultrasonic dispersion and heavy liquid GPS-V (a concentrated aqueous solution of sodium heteropolytungstate) (for details see in (Silantiev et al 2024)).

Zircon Dating by Chemical Abrasion–Isotope Dilution–Thermal Ionisation Mass Spectrometry. Selected zircon grains (ca. 30–50 grains with most idiomorphic forms) were annealed at 900 °C for 96 h and then chemically abraded at 210 °C for 12 h (sample I-22) and 14 h (sample I-12) with concentrated HF and HNO_3 in a pressurised Parr dissolution vessel. This procedure dissolves crystal domains suspected of post-crystallisation lead loss by causing severe radiation damage (Mattinson, 2005).

The acid was then completely pipetted out together with the dissolved zircon material and 3.5N HNO_3 was added to the remaining zircon grains and fragments and left for 30 min at 50 °C to remove surface lead. Several cleaning cycles with water combined with repeated ultrasonic treatment were carried out before individual zircon fragments were selected for further processing. Individual zircon

 doi:10.20944/preprints202407.1814.v1

grains/fragments were washed with 3.5 N HNO_3 and transferred into clean microcapsules with a small drop of this liquid and four drops of concentrated HF. Samples were spiked with a ^{205}Pb-^{233}U-^{235}U- tracer solution (ET535 at TU Bergakademie Freiberg) (Condon et al., 2015). For final dissolution, the microcapsules were placed in pressurised Parr dissolution vessels and heated to 200 °C for 48 h, followed by drying at 130 °C and then redissolving in 6N HCl for 24 h at 200 °C to convert to chlorides. After repeated drying, the samples were dissolved in ten drops of 3.1 N HNO_3 and transferred into microcolumns for column chemistry. The U and Pb were separated from the rest of the sample by anion exchange chromatography using HCl and H_2O. The U and Pb containing fraction was applied to pre-degassed rhenium filaments with a drop of silica gel (Gerstenberger and Haase, 1997) and measured on an IsotopX Phoenix Mass Spectrometer using a SEM Daly ion counter.

The accuracy of the dating results was checked by repeated measurement of zircon standards 91500 (Wiedenbeck et al., 1995) and Temora 2 (Black et al., 2004). The published ages of Temora 2 were determined as 416.8 ± 0.3 Ma (Black et al., 2004) and 417.35 ± 0.05 Ma (Schaltegger et al. 2021). Our date of 417.3 ± 0.6 Ma (Käßner et al., 2021) is in perfect agreement with these values. Zircon standard 91500 was dated to 1062.4 ± 0.4 Ma (Wiedenbeck et al., 1995) or 1063.6 ± 0.3 Ma (Schoene et al., 2006). Our weighted mean $^{206}Pb/^{238}U$-age of 1064.6 ± 1.3 Ma was within 0.1% of the accepted values. Based on the standard dating results, we consider the present CA-ID-TIMS ages to be accurate at the 0.1% level.

5. Results

Petrography of tonsteins. An analysis of the structural features and mineralogical composition of tonsteins was conducted with an optical microscope in thin sections. The tonsteins represent a silty-clayey rock devoid of primary lamination (see Figure 11). The main mass of the rock is composed of kaolinite, including clusters and phenocrysts of organic matter. Kaolinite is represented by a range of forms, including cryptocrystalline mass, individual crystals, aggregates of crystals, as well as pseudomorphoses on feldspars and mica. The significant organic matter content is confirmed by the rather high Loss on Ignition (LOI) values of 35.6 (tonstein I-12) and 13.6 (tonstein I-22) (Table 1). The silty-clayey mass comprises a large number of angular crystals and grains of quartz and feldspar. The lack of lamination is further evidenced by the non-oriented arrangement of mineral grains, crystal aggregates, and clots of organic matter (Figure 11A, B).

X-ray diffraction (XRD) analysis confirms the mineral composition established by petrographic studies. Tonsteins are predominantly composed of kaolinite (42.5–56.2%) and quartz (22.9–35.0%) (Table 1), with subordinate contents of K–feldspars (sanidine and microcline) (9.8–12.5%), albite (4.2–5.6%) and apatite (2.7–11.8%).

 doi:10.20944/preprints202407.1814.v1

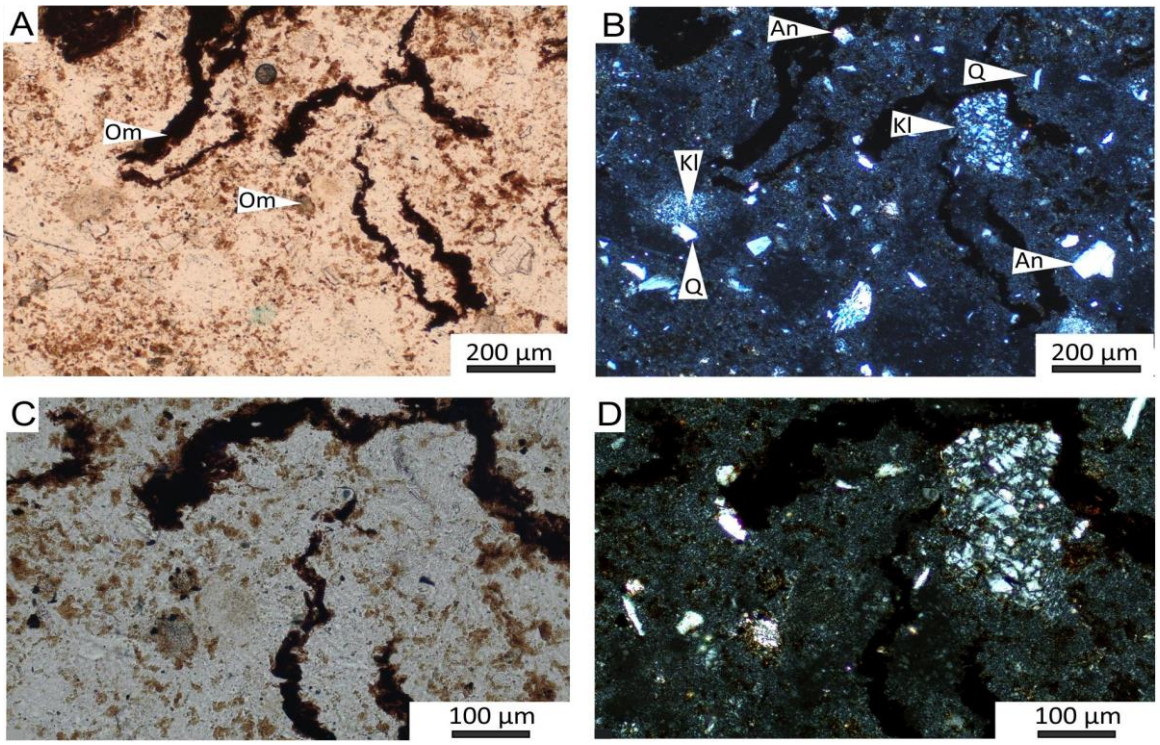

Figure 11. Tonstein structure in thin section: A – homogeneous cryptocrystalline mass of kaolinite with clusters and phenocrysts of organic matter (Om); B – the same in crossed nicols: An – anorthoclase; Kl – aggregates of kaolinite crystals; Q - quartz; C, D – the same section in higher magnification; D – in crossed nicols. Tonstein I-12.

Table 1. Mineral composition of the studied tonsteins, %.

Mineral	tonstein I-12	tonstein I-22
Kaolinite	42.6	56.2
Quartz	35.0	22.9
K-feldspar (sanidine and microcline)	9.8	12.5
Albite	4.2	5.6
Apatite	11.7	2.7
Total	99.1	99.9

Scanning electron microscopy/energy-dispersive X-ray spectrometry (SEM-EDS) of tonsteins enables the detection and identification of sparsely distributed and accessory mineral phases and significantly complements the list of minerals established by XRD analysis.

Tonstein I-12 contains, in addition to the minerals listed in Table 1, sphalerite, celestine, barite, fluoroapatite, brass with lead nugget inclusions, illite, ilmenite (pseudorutile), and baddeleyite.

Tonstein I-22 contains, in addition to the minerals listed in Table 1, zinc nuggets, sphalerite, pyrite, pyrite with nickel admixture, montmorillonite, anorthoclase, barite, and celestine. According to previous studies (Vergunov et al., 2024), tonstein I-22 also includes Zr-bearing minerals represented by zircon, baddeleyite and complex Ca-Nb-Zr-P silicates of variable composition, as well as lanthanides (monazite) and nodular sulphides (galena and sphalerite).

Major elements of tonsteins determined by Inductively coupled plasma atomic emission spectroscopy (ICP-AES). The content of rock-forming oxides in tonsteins I-12 and I-22, and their

 doi:10.20944/preprints202407.1814.v1

average composition in post-Archean upper continental crust (UCC) (Rudnick and Gao, 2014) and shales (Gromert et al., 1984) are summarised in Table 2.

Tonstein I-12 has TiO_2, Al_2O_3, and CaO contents close to the average chemical composition, with the exception of P_2O_5, which is more than an order of magnitude higher. The contents of other major element oxides are lower than the average values: SiO_2 is approximately half the average, and Fe_2O_3, MnO, MgO, K_2O, and Na_2O are almost an order of magnitude lower. Tonstein I-22 has elevated values of Al_2O_3 and P_2O_5, while the TiO_2 content is close to the average composition values. The contents of other major element oxides are lower than the average composition values.

The low contents of most rock-forming oxides in the studied tonstein samples are associated with a significant content of LOI (loss on ignition), primarily due to the presence of organic matter. Upon recalculating the data for inorganic matter, it is evident that the tonsteins are significantly enriched in TiO_2, Al_2O_3, CaO and P_2O_5. The increase of alumina and titanium oxides concentrations is attributed to the loss of the elements, particularly of silica, potassium and sodium, which occurred during the transformation of parent ash material into tonstein. The concentrations of CaO and P_2O_5 are associated with the presence of stable fluorapatite in the source material. The recalculated content of rock-forming oxides aligns well with the mineral composition shown in Table 1. The reduced contents of most rock-forming oxides suggest that the tonsteins, derived from volcanic ash material, are geochemically distinct from basin sedimentary rocks, which predominantly consist of clastic material supplied from source areas.

Table 2. Content of major element oxides in the studied tonsteins determined by ICP-AES (Vergunov et al., 2024).

Major element oxides (weight %)	I-12	I-22	UCC	NASC
SiO2	34.7	49.8	66.6	64.8
TiO2	0.59	0.65	0.64	0.70
Al2O3	16.4	27.8	15.4	16.9
Fe2O3	0.81	0.86	5.61	6.30
MnO	0.011	0.006	0.10	0.06
CaO	3.61	1.58	3.59	3.63
MgO	0.20	0.31	2.48	2.86
K2O	0.85	0.71	2.80	3.97
Na2O	0.18	0.37	3.27	1.14
P2O5	2.16	0.88	0.15	0.13
Loss on Ignition (LOI, %)	35.6	13.6	-	-
Total	99.7	99.8	100.64	100.49
SiO_2/Al_2O_3	2.12	1.79	4.3	3.8
TiO_2/Al_2O_3	0.036	0.023	0.042	0.041

Note. All oxide values are in weight %. Average chemical composition: UCC – upper continental crust, post-Archean (Rudnick and Gao, 2014), NASC – North American Shale Composite (Gromert et al., 1984); the orange colour indicates increased values while the blue colour indicates decreased values; values close to the average content are not coloured.

The SiO_2/Al_2O_3 ratio in the studied tonsteins ranges from 1.79 (tonstein I-22) to 2.12 (tonstein I-12), and the TiO_2/Al_2O_3 ratio from 0.036 (tonstein I-22) to 0.023 (tonstein I-12). These values are lower

 doi:10.20944/preprints202407.1814.v1

than these ratios for average chemical composition. The lower SiO_2/Al_2O_3 ratio compared to the average chemical composition indicates silica removal during ash kaolinisation, and the lower TiO_2/Al_2O_3 ratio indicates the acid (rhyodacite) composition of the primary ashes (Spears, 2012).

Trace elements of tonsteins obtained by the ICP-MS method. The contents of trace elements in the studied tonsteins, the average contents in sedimentary rocks (Grigoriev, 2002, 2003), in the post-Archean upper continental crust (UCC) (Rudnick and Gao, 2014), in acid volcanic rocks (Grigoriev, 2002, 2003), and in coal ashes (Ketris and Yudovich, 2009) are summarised in Table 3[1].

Tonstein I-12 contains elevated concentrations of Li, Be, Cu, Zn, Ga, Ge, As, Se, Y, Ce, Nd, Sm, Eu, Gd, Tb, Dy, Ho, Er, Tm, Yb, Lu, and Th compared to the average composition of sedimentary rocks and UCC. Conversely, this tonstein shows reduced contents of V, Cr, Co, Ni, Rb, Zr, Cs, W, and Tl. The concentrations of Sc, Sr, Nb, Mo, Cd, Sn, Sb, Ba, Hf, Ta, and U are close to average values for sedimentary rocks and UCC.

Tonstein I-22 contains elevated concentrations of Ni, Cu, Zn, Ga, Ge, As, Se, Y, La, Ce, Pr, Nd, Sm, Eu, Gd, Tb, Dy, Ho, Er, Yb, Hf, Ta, Pb, Th, and U. Reduced contents are noted for Li, Be, V, Cr, Co, Rb, Zr, Cs, Ba, Tm, W, and Tl. The concentrations of Sc, Sr, Nb, Mo, Cd, Sn, Sb, and Lu are close to average values for sedimentary rocks and UCC.

Table 3. Trace elements (ppm) in the studied tonsteins and average concentrations in relevant rocks.

Element	Tonstein I-12	Tonstein I-22	Sedimentary rocks[1]	Upper continental crust (UCC)[2]	Acid volcanic rocks[3]	Coal ashes[4]
Li	68.2	20.7	33	21	26	66
Be	4.3	0.45	1.9	2.1	4	9.4
Sc	11.4	6.9	9.6	14	4.2	23
V	8.4	11.9	91	97	60	155
Cr	2.4	3.4	58	92	8.5	100
Co	1.3	1.7	14	17.3	4.8	32
Ni	21.9	92.2	37	47	8	76
Cu	68.6	57.5	31	28	15	92
Zn	100.4	55.7	43	67	35	140
Ga	20.8	36.2	12	17.5	26	33
Ge	9.2	14.9	1.4	–	1	15
As	14.9	10.8	7.6	–	4.3	47
Se	6.4	8.1	0.27	–	0.093	8.8
Rb	14.6	8.4	94	84	190	79
Sr	236	218	270	320	240	740
Y	81.2	39.2	29	21	24	51

[1] It should be noted that the values in Table 3 are given for the original samples without LOI. If the correction coefficients are introduced, then all values indicated for tonstein I-12 increase by a factor of 1.55, and for tonstein I-22 by a factor of 1.16. This increase does not affect the results discussed herein.

 doi:10.20944/preprints202407.1814.v1

Zr	94.8	115.3	170	193	110	210
Nb	7.1	4.6	7.6	12	26	20
Mo	1.4	1.2	1.5	–	3.4	14
Cd	0.3	0.2	0.8	0.09	0.3	1.2
Sn	2.1	3.0	2.9	2.1	3.5	6.4
Sb	0.1	0.70	1.2	0.4	–	6.3
Cs	0.6	0.9	7.7	4.9	10	6.6
Ba	445	231	410	628	480	940
La	35.6	88.1	32	31	31	69
Ce	76.9	169.8	52	63	58	130
Pr	8.7	16.7	6.8	7.1	10	20
Nd	35.5	62.0	24	27	27	67
Sm	7.9	10.8	5.5	4.70	5.2	13
Eu	1.8	1.6	0.94	1.0	1.5	2.5
Gd	8.6	9.8	4	4.0	5	16
Tb	1.3	1.4	0.69	0.70	0.82	2.1
Dy	8.8	7.4	3.6	3.90	6	14
Ho	2.1	1.4	0.92	0.83	1.7	4.0
Er	7.3	3.4	1.7	2.30	3.6	5.5
Tm	1.1	0.5	0.78	0.30	1	2.0
Yb	8.0	3.0	2.0	1.96	2.5	6.2
Lu	1.1	0.4	0.44	0.31	0.55	1.2
Hf	3.9	5.2	3.9	5.3	4.1	8.3
Ta	0.9	1.9	1.0	0.9	1.8	1.7
W	0.5	0.3	2.0	–	1.4	6.9
Tl	0.13	0.07	0.89	0.9	2.1	4.9
Pb	19.7	30.0	12	17	23	47
Th	12.29	31.90	7.7	10.5	13	21
U	3.8	7.1	3.4	2.7	4.5	16
Th/U	3.2	4.5	2.26	3.9	2.9	1.3

Note. All values are in ppm. Average trace element content: [1, 3] – Grigoriev (2002, 2003); [2] – (Rudnick and Gao, 2014); [4] – (Ketris and Yudovich, 2009); the orange colour indicates increased values while the blue colour indicates decreased values; values close to the average content are not coloured.

The values of some elements recorded in tonsteins I-12 and I-22, both elevated (Be, Ga, Eu, Dy, Er, Tm, Ta, Th) and reduced (Li, V, Cr, Co, Ni, Zr), correlate with the average contents in acid volcanic

 doi:10.20944/preprints202407.1814.v1

rocks. Elevated values of elements such as Li, Ni, Cu, Ga, Ge, Se, Y, REE, Hf, Ta, Pb, Th, and U also correlate with concentrations of these elements in coal ash.

General Description of Zircon Crystals. The study of zircon grain populations from tonstein I-22 (60 grains) and tonstein I-12 (100 grains) using optical and scanning electron microscopes revealed in both cases the predominance of medium prismatic crystals (60% and 45%, respectively), with length-to-width ratios ranging from 2 to 4. Short prismatic crystals, with length-to-width ratios less than 2, are subdominant, accounting for 30% and 35%, respectively. Long-prismatic crystals, with a length-to-width ratio greater than 4, account for 10% and 20%, respectively. Most grains (about 85%) have well developed {101}–{211} pyramids. Photographs of crystal populations and individual grains are shown in Figures 9, 12 and 13.

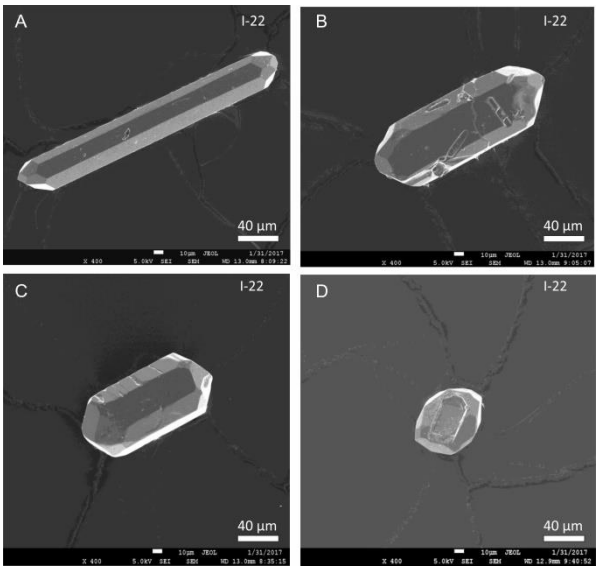

Figure 12. Zircon grains from tonstein I-22: (A) – long prismatic crystal; (B) – medium prismatic crystal; (C, D) – short prismatic crystals; SEM-photos.

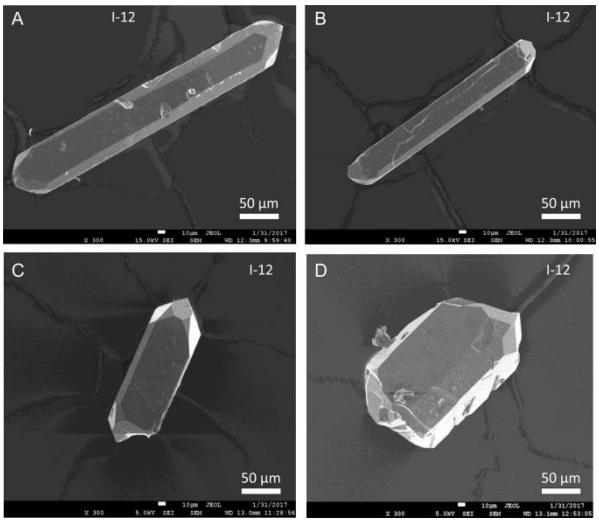

Figure 13. Zircon grains from tonstein I-12: (A, B) – long prismatic crystals; (C) – medium prismatic crystal; (D) – broken crystal; SEM-photos.

Transparent crystals predominate (more than 55%) in both tonsteins I-22 and I-12. They are either colourless (about 25%) or have yellowish (about 15%) or brownish (about 15%) shades. Opaque muddy crystals account for 45% and are mostly coloured in yellowish and brownish shades; opaque colourless crystals are very rare (2%). In general, zircon grain populations from tonsteins I-22 and I-12 contain approximately 75% idiomorphic grains of good preservation. Rounded grains account for

Preprints.org (www.preprints.org) | NOT PEER-REVIEWED | Posted: 23 July 2024 doi:10.20944/preprints202407.1814.v1

4–5%, grains with broken edges and faces account for 5–6%, grains with intense fracturing account for about 10% and finally at least 5% of the grains contain well-defined inclusions.

Morphological Features of Zircon Crystals. Zircon grains from tonsteins I-22 (60 grains) and I-12 (100 grains) were subdivided into main types and secondary subtypes according to the methodological approach of J.P. Pupin (1980). The resulting data are shown in Figures 14 and 15, based on the diagram of morphological features of zircon crystals (Pupin, 1980) (see Methods section, Figure 10).

In tonstein I-22 (Figure 14), the most prevalent zircon grains represent main type S ({100}–{110} prisms, {101}–{211} pyramids), among which subtypes S_{17} and S_{18} dominate (about 55%), while subtypes S_{23} and S_{25} subdominate (in total about 25%), and the number of other subtypes is of minor value. Scattered grains of subtype P_5 ({100}–{110} prisms, {101} pyramids) and subtypes Q_4 and Q_5 ({100}–{110} prisms, {211} pyramids) are also recorded.

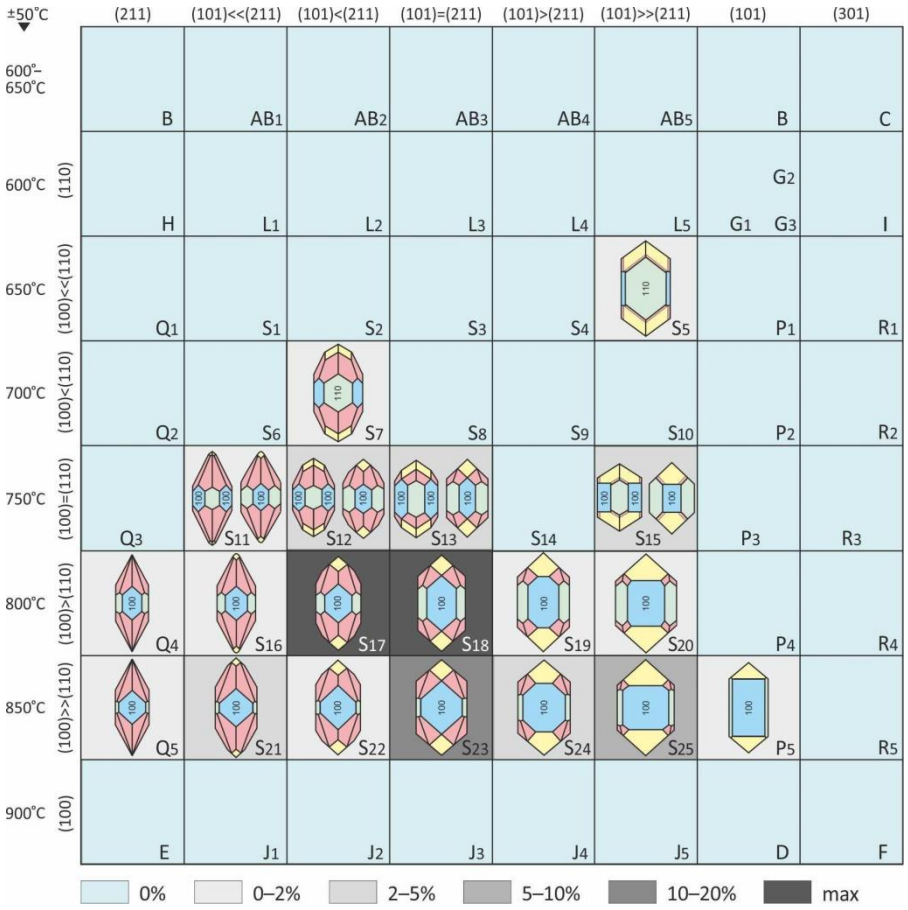

Figure 14. Quantitative distribution of zircon grain morphotypes from tonstein I-22 according to the diagram of Pupin (1980); morphotypes S_{17} and S_{18} with developed prismatic facets {100} predominate.

In tonstein I-12 (Figure 15), the same main types P, Q, S, as in tonstein I-22, occur. Subtypes S_{18} and S_{19} (about 60%) are dominant, subtype S17 (about 15%), and subtypes P_4, Q_4, and S_{20} (totally about 20%) are subdominant; while the remaining six subtypes (Q_2, Q_3, S_9, S_{12}, S_{14}, P_5) are represented by single grains.

 doi:10.20944/preprints202407.1814.v1

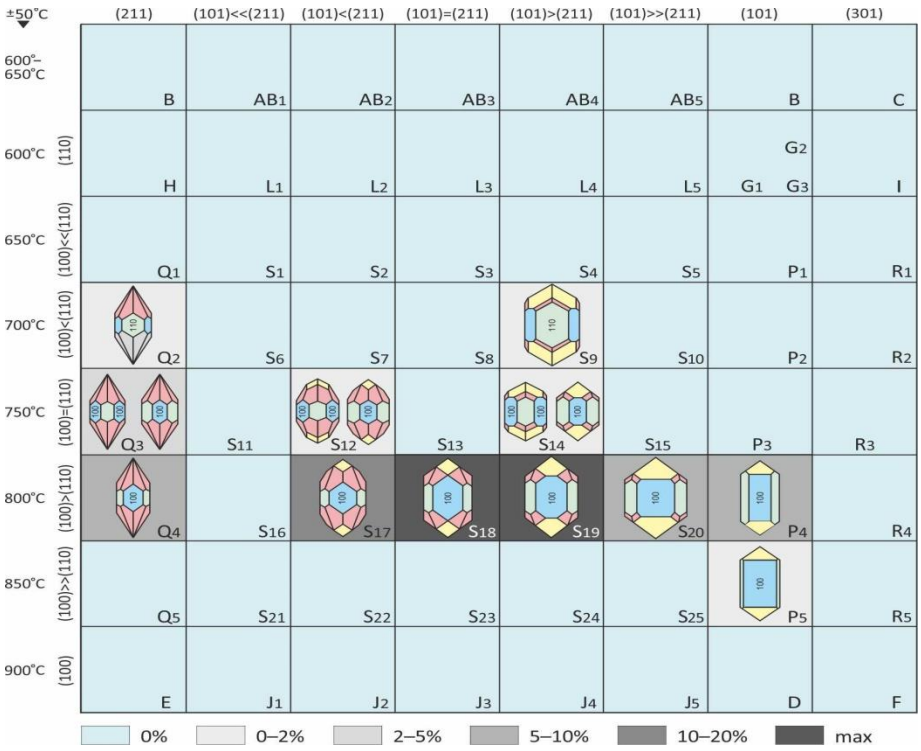

Figure 15. Quantitative distribution of zircon grain morphotypes from tonstein I-12 according to the diagram of Pupin (1980); morphotypes S_{18} and S_{19} with developed prismatic facets {100} predominate.

In general, both tonsteins contain crystals of the main types P, Q, S, among which the subtypes S_{17}, S_{18}, S_{19} dominate. The morphological subtypes are grouped in the lower part of the diagram (Pupin, 1980), suggesting that the crystallisation conditions of most crystals were similar.

The Results of the Cathodoluminescence Study revealed that most of the zircon grains extracted from tonsteins I-22 and I-12 have complex zonality, both parallel-symmetric and asymmetric. Analysis of the cathodoluminescence images enabled us to exclude grains with mechanical disturbances and asymmetric zonality from radioisotope dating, as these features indicate the probable occurrence of an older crystalline core.

Study of Melt Inclusions. Examination of the internal structure of zircon grains extracted from tonsteins I-22 and I-12 indicates the presence of crystalline, vitreous, and gas-fluid melt inclusions (Figure 16) (personal communication Anatoliy G. Nikolaev, Kazan Federal University). The presence of melt inclusions with gaseous phase indicates rapid cooling of the primary crystal growth medium and is consistent with geochemical data on the accumulation of tonsteins from volcanic ash falls.

 doi:10.20944/preprints202407.1814.v1

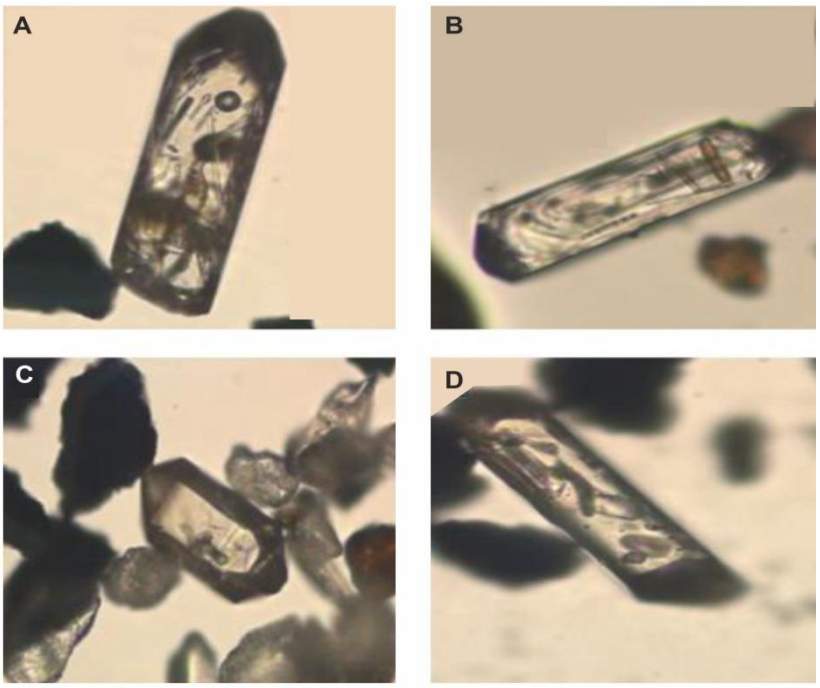

Figure 16. Zircon grains with melt inclusions: A – crystal containing melt inclusions with gaseous phase, indicating rapid cooling of the primary crystal growth medium, B – crystal containing crystalline inclusion; well-defined zonality of the crystal is visible; C – crystal containing vitreous inclusion; D – crystal containing vitreous and gas-fluid melt inclusions; A, B – grains from tonstein I-12; C, D – grains from tonstein I-22.

Analysis of melt inclusions in zircons extracted from the tonsteins I-22 and I-12 indicates a crystallisation temperature range of 700–900 ºC, which is in general agreement with the results of the morphological study of zircon crystals.

Results of Radioisotopic Dating. Zircon U-Pb CA-ID-TIMS isotopic results are shown as $^{206}Pb/^{238}U$ ranked age plots in Figure 17. Mean sample ages representing crystallisation were calculated from established age clusters with the software ET Redux (Bowring et al., 2011). The error of weighted mean ages is given as $\pm x/y/z$, where x is the internal 2σ measurement error; y is the internal 2σ error plus tracer calibration uncertainty; and z additionally includes the uncertainty of the decay constant. For discussion, we use the z-error, which includes the internal 2σ measurement error, the tracer calibration uncertainty and the uncertainty of the decay constant and enables comparison with other dating methods.

For the sample from tonstein I-22, 10 zircon fragments were dated. The single zircon ages vary from 258.1 to 265.5 Ma and often have a high measurement error due to the small size of remaining zircon fragments. Six measurements form a cluster with similar ages between 259.8 and 262.8 Ma. These measurements were used to calculate a weighted mean age of 261.4 ± 0.7 Ma (MSWD = 2.7). Two other zircon fragments show older ages, which represent inherited components (e.g., xenocrystic cores) whereas two younger ages represent slight Pb loss.

 doi:10.20944/preprints202407.1814.v1

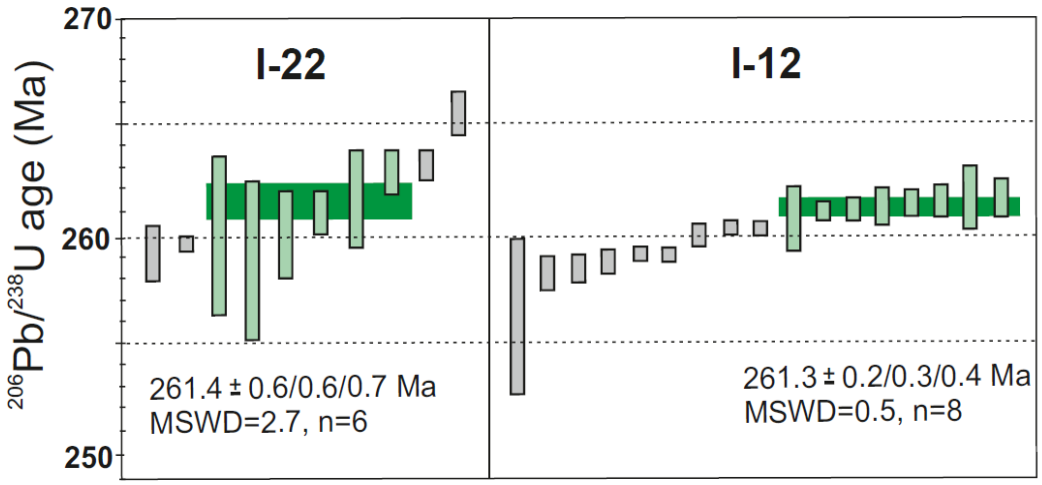

Figure 17. Ranking plot of $^{206}Pb/^{238}U$ dates from single grains of zircon from I-22 and I-22 tonsteins analysed using CA-ID-TIMS; Izykh Fm, Guadalupian, Middle Permian. A weighted mean date is represented by the green boxes behind the error bars. Abbreviations: MSWD—mean square of weighted deviations; n—number of zircon grains dated.

For sample from tonstein I-12, we dated 17 zircon fragments. The single zircon ages vary from 257.1 to 261.7 Eight measurements form a cluster with similar ages between 260.7 and 261.7 Ma. These measurements were used to calculate a weighted mean age of 261.3 ± 0.4 Ma (MSWD = 0.5). All other zircon fragments show younger ages, which represent slight Pb loss.

6. Discussion

Petrography of tonsteins. Tonsteins, consisting mainly of cryptocrystalline and recrystallised kaolinite, and its pseudomorphs after other minerals, are widely known from coal-bearing basins of different ages (Zaritsky, 1967; 1985; Spears 1970, 2012; Loughnan, 1978; Chernovyants, 1992; Bohor and Triplehorn, 1993). The formation of kaolinite is thought to be due to its diagenetic mineralisation from parent volcanic ash falls under acidic conditions caused by the accumulation and humification of thick peats (Demchuk and Nelson-Glatiotis 1993). The significant amount of organic matter indicates that the burial of the primary sediment, which captured organic matter, occurred rapidly enough and under conditions where biota could not destroy it. The rapid accumulation of matter is confirmed by the presence of angular crystals of quartz and feldspar, as well as by the absence of rock lamination and unoriented arrangement of mineral grains.

X-ray diffraction (XRD) and scanning electron microscopy/energy dispersive X-ray spectrometry (SEM-EDS) confirm the mineral composition of the tonsteins established by petrographic studies. The alkaline feldspars, sanidine, albite and anorthoclase, are considered relict minerals of primary volcanic ash. Sanidine ($K(AlSi_3O_8)$), the highest temperature (650–800°C and above) potassium feldspar, is a typical mineral of intermediate to acidic volcanic rocks, particularly for rhyolite and trachyte fallout ash beds. Albite ($NaAlSi_3O_8$) and sanidine form a continuous series of solid solutions, so their co-occurrence in the tonstein is quite appropriate and indicates a sufficient amount of sodium in the parent material. Anorthoclase ($(Na,K)AlSi_3O_8$), has an intermediate composition in the continuous series of sanidine and albite. It was first described from a locality on the Pantelleria Island, Sicily, and is characteristic of high temperature (above 600 °C) sodium-rich volcanic rocks. Thus, its presence in tonstein is a direct indication of the pyroclastic nature and high alkalinity of the parent material.

The alkaline (pantellerite-comendite) composition of the primary ash material is also confirmed by the occurrence of low-stable complex zirconium-silicate minerals in association with leach-resistant zircons (Vergunov et al., 2024). The presence of Zr-bearing minerals comprising zircon,

 doi:10.20944/preprints202407.1814.v1

baddeleyite and complex Ca-Nb-Zr-P silicates of variable composition, along with the occurrence of lanthanides (monazite) and nodular sulphides (galena and sphalerite), suggests that the parent material, which was subsequently transformed into kaolinite and associated tonstein minerals, could have been derived from synchronous volcanic inputs (e.g. air-fall ash) (Bohor and Triplehorn, 1993; Burgers et al., 2000; Spears, 2012; Arbuzov et al., 2016; Dai et al., 2017;Vergunov et al., 2024).

Major elements of tonsteins determined by Inductively coupled plasma atomic emission spectroscopy (ICP-AES). The tonsteins I-12 and I-22 are predominantly composed of SiO_2 and Al_2O_3, which in total exceed 50% (Table 2). The elevated SiO_2/Al_2O_3 ratio of 2.12 in tonstein I-12 is consistent with the increased silicification of the rock (Vergunov et al 2024). The lower SiO_2/Al_2O_3 value of 1.79 in tonstein I-22 is in agreement with the predominance of kaolinite in its composition.

The TiO_2/Al_2O_3 ratio (Table 2) is often used as an auxiliary criterion of the contribution of pyroclastics to coal accumulation (Yudovich and Ketris, 2000) and for reconstructing the original composition of altered ash material (Dai et al., 2017). It is assumed that the value of TiO_2/Al_2O_3 ratio below 0.02 is characteristic of rhyolitic pyroclastics (Spears and Kanaris-Sotiriou, 1979).

The TiO_2/Al_2O_3 value for tonstein I-22 is 0.023, which may be evidence of the proximity of the original ash matter to rhyolitic pyroclastics (Vergunov et al 2024). A TiO_2/Al_2O_3 ratio between 0.02 and 0.06 indicates the contribution of intermediate or alkaline volcanic ash (Spears and Kanaris-Sotiriou, 1979). The TiO_2/Al_2O_3 value for tonstein I-12 is 0.036, which provides further confirmation that the parent matter was similar in composition to this type of volcanic ash.

Trace elements of tonsteins obtained by the ICP-MS method. The majority of trace elements in tonsteins I-12 and I-22 demonstrate comparable trends of change (increase or decrease) in concentrations compared to average contents (Table 3). Both tonsteins display an increase in most REEs (Sc, Y, and lanthanides). At the same time, the concentrations of some elements (e.g., Li, Be, Ni) exhibit multidirectional trends, with one tonstein showing an increase and the other a decrease compared to the average contents. A third group of elements, including La, Pr, Hf, Ta, and U, which have increased values in tonstein I-22, and in tonstein I-12 their contents are close to the average contents, is also distinguished. The differences in the content of chemical elements in the tonsteins can be attributed to the different composition of the parent volcanic ash (Vergunov et al., 2024).

Previous studies of the studied tonsteins, in particular the study of the Eu anomaly and Zr/TiO2-Nb/Y diagram (Vergunov et al., 2024), led to the conclusion of more acidic, rhyolite-pantellerite, parent pyroclastics in the tonstein I-22 and more basic, dacite-rhyodacite, pyroclastics in the tonstein I-12.

Zircons. The good preservation and idiomorphic crystallographic outlines of the majority (about 75%) of the zircon grains extracted from tonsteins I-22 and I-12 indicate that in both cases we are dealing with monomineral populations, each formed from a single magmatic melt. The dominance of subtypes S17, S18, and S19 of the main type S ({100}–{110}, {101}–{211}), the presence of long prismatic crystals of subtypes P4 ({100}>{110}) and P5 ({100}>>>{110}), the grouping of morphotypes in the lower part of the J. P. Pupin's diagram of (Figures 14, 15), confirms the homogeneity of the mineral populations and suggests similar conditions for the growth of most crystals in the temperature range 750–850 ºC.

The crystallisation temperature of zircons from tonsteins I-22 and I-12 in the range 700-900 ºC is confirmed by the analysis of melt inclusions. The small number of crystals with well-defined {110} facets crystallising at relatively lower temperatures is also consistent with this temperature range. There is evidence that, in addition to temperature, the growth medium has an influence on the morphology of zircon crystals (Benisek and Finger, 1993); this suggestion requires further investigation.

These results are generally consistent with the general pattern of magmatic melt formation, where silica-rich acidic melts have a temperature range of 700–900 ºC, whereas basic melts enriched in alkali and rare earth oxides have higher temperatures, typically above 900 ºC (Ghiorso & Sack, 1995; Annen & Zellmer, 2008). Despite the fact that in both tonsteins the dominant morphotypes of zircon crystals are subtypes forming at 800 ºC, a trend of a slight increase in crystallisation temperature from the lower to the upper tonstein can be observed. Thus, tonstein I-22, which is

 doi:10.20944/preprints202407.1814.v1

thought to have formed from rhyolitic parent ash, includes six low-temperature morphotypes with crystallisation temperatures of 650–750ºC; whereas tonstein I-12, formed from intermediate or alkaline volcanic ash, contains only five low-temperature morphological subtypes, with crystallisation temperatures not lower than 700–750ºC.

In general, the petrography, mineral composition, and geochemical data of the tonsteins are in good agreement with the results of the morphological study of zircon crystals and the analysis of melt inclusions, indicating the formation of the parent ashes of the studied tonsteins and associated minerals from synchronous volcanic inputs (e.g., air-fall ash) derived from rhyolite-pantellerite (tonstein I-22) and dacite-rhyodacite (tonstein I-12) magmatic melts with temperatures of 700–900ºC.

Radioisotopic dating versus biostratigraphy. Radioisotopic weighted mean ages of 261.4 ± 0.7 Ma (MSWD = 2.7) (tonstein I-22) and 261.3 ± 0.4 Ma (MSWD = 0.5) (tonstein I-12) (Figures 7 and 17) indicate that the host strata (coal seams XXX and XXX^{a}; middle part of the Izykh Fm) belong to the Capitanian Stage of the International Chronostratigraphic Chart (International..., 2023) or to the Severodvinian Stage in terms of the General Stratigraphic Scale of Russia (GSSR) (Stratigraphic Guide.., 2019) (Figure 2). At the same time, the biostratigraphic age of this interval is accepted nowadays as Roadian (Kazanian, GSSR) (Sivtchikov and Donova, 2016; Fedotov et al., 2019). Thus, our dating suggests that the Izykh Fm is about 10 Ma younger than currently thought.

It should be noted that a direct correlation of the biostratigraphic data of the Minusinsk Basin with the subdivisions of the GSSR is impossible, because on the one hand the Angarida, which includes the Minusinsk Basin and other basins of modern Siberia, and on the other hand the East European Platform and the Cis-Uralian Foredeep, the stratotype region of the GSSR stages, belong to different phytogeographic and zoogeographic provinces (Schneider et al. 2020; Silantiev et al. 2024). For this reason, the biostratigraphic age of the lithostratigraphic units of the Minusinsk Basin is determined by comparing their palaeontological and palaeobotanical assemblages with those of the Kuznetsk Basin, which serves as the adopted biostratigraphic standard (Budnikov, 1996; Budnikov et al., 2020). Therefore, in Figure 2, the units of the Minusinsk Basin are correlated with the formations of the Kuznetsk Basin, and we will use these formations in further characterising the palaeobotanical features of the Izykh flora. It should be noted that the biostratigraphic standard of the Kuznetsk Basin is very conventionally correlated with the GSSR subdivisions and is essentially contractual, requiring constant refinement (for examples of refinement see (Davydov et al., 2021; Silantiev et al., 2023, 2024)).

The rich collections of plant remains from the shale package overlying coal seam XXX were examined by Sivtchikov and Donova (2016), who provided the following list of taxa (unfortunately without illustration): *Phyllotheca* (*Equisetinostachys*) *grandis* (Gorel.) S. Meyen, *Ph. equisetitoides* Schm., *Ph.* cf. *turnaensis* Gorel., *Glottophyllum elongatum* Radcz., *Cordaites gorelovae* S. Meyen, *C.* cf. *gracilentus* (Gorel.) S. Meyen, *C. clercii* Zal., *C. kuznetskianus* (Gorel.) S. Meyen, *C. minax* (Gorel.) S. Meyen, *C. radczenkoi* (Gorel.) S. Meyen, *C. truncatus* S. Meyen, *Cordaites* typ. *concinnus* (Radcz.) S. Meyen, *Rufloria* sp., *R.* cf. *brevifolia* (Gorel.) S. Meyen, *Crassinervia* cf. *iljinskiensis* Radcz., *Niazonaria* sp, *Samaropsis borisovaensis* Such., *S.* (?) aff. *saggatiformis* Such., *Cordaicarpus* sp., *Tungussocarpus* ex gr. *tychtensis* (Zal.) Such., *T.* cf. *rotundatus* (Such.) Such., *Sylvella dubia* (Neub.) Neub. According to the authors, this assemblage, which combines *Rufloria* and *Cordaites* with the upper surface of the leaves striated with numerous small furrows masking the veining, is characteristic of the Ilyinskoe Subgroup (Kazankovo-Markina and Uskat Fms) of the Kuznetsk Basin. In the approved Stratigraphic Scheme of the Kuzbass, the Ilyinskoe Subgroup is compared with the Kazanian Stage of the GSSR, which in turn is correlated with the Roadian Stage of the ICC (Schneider et al., 2020).

In the opinion of L.G. Porokhovnichenko (this paper), the taxonomic composition of the assemblage reported by Sivtchikov and Donova (2016) indicates that it belongs to the so-called Kolchugino flora in the time range of the Ilyinskoe Subgroup (Figure 2). This is supported by a number of reliable taxa: *Tungussocarpus tychtensis* (appears only from Ilyinskoe Subgroup of the Kuzbass and occurs in the interval including Kazankovo-Markina Fm and Gramoteino Fm); *Tungussocarpus rotundatus* (Kazankovo-Markina Fm and Leninsk Fm); *Sylvella dubia* (Usa Beds and Erunakovo Subgroup); *Glottophyllum elongatum* (Kazankovo-Markina Fm and Leninsk Fm); *Rufloria brevifolia* (Kazankovo-Markina Fm and Uskat Fm); *Cordaites clercii* Zal. (uppermost Uskat Fm and

 doi:10.20944/preprints202407.1814.v1

Erunakovo Subgroup); *C. gorelovae* (Kuznetsk Subgroup and Leninsk Fm); *C. gracilentus* (Kuznetsk Subgroup and lower Leninsk Fm).

It is crucial to note that, among the species mentioned above, only *Rufloria brevifolia* is limited in its distribution to the Kazankovo-Markina and Uskat Fm (= Roadian). In contrast, the other species have a more extensive stratigraphic ranges, which span the overlying Leninsk and Gramoteino Fm of Erunakovo Subgroup (= Wordian-Capitanian). In addition, the list contains *Cordaites clercii*, a species occurring exclusively in the Erunakovo Subgroup. Assuming there was an error in the determination of *Rufloria brevifolia* (e.g., due to poor preservation of the specimen), the remaining floristic assemblage does not contradict the new radioisotopic dating. It is important to note that this issue can only be resolved with additional sampling and re-examination of previously collected plant remains from the Izykh Fm.

The Upper Narylkova Subformation (Sfm) underlying the Izykh Fm is compared by floristic remains to the Ishanova and Kemerovo Fms of the Kuznetsk Basin (upper Balakhonka Subgroup = Artinskian-Kungurian) (Sivtchikov and Donova, 2016). This suggests a hiatus in sedimentation spanning at least 5 Ma, i.e. the time interval of the Kuznetsk Subgroup (upper Kungurian of ICC or Ufimian of GSSR) (Figure 2).

The conclusion of a long hiatus in sedimentation is unusual for the geology of the coal-bearing Upper Palaeozoic of the southern Angaraland. This succession, at least in the reference Kuznetsk Basin, is considered to be continuous, with only one distinct unconformity at the boundary of the Balakhonka and Kolchugino Groups (Gorelova, Budnikov, 1996; Yarkov, 1996; Betekhtina et al., 1998); and the temporal extent of this unconformity is considered to be much smaller than the recognised biostratigraphic units.

Viktor Sivtchikov (Sivtchikov and Donova, 2016) was the first to comment on the significant role of unconformities in the coal-bearing sequence of the Minusinsk Basin, justifying the gap between the Izykh and Narylkova Fms, and between the Narylkova and Beliy Yar Fms on the basis of palaeobotanical data, and suggesting the presence of a discontinuity within the Narylkova Fm. We agree with Sivchikov (Sivchikov and Donova, 2016, p. 23) that insufficient attention of palaeontologists to the possible hiatus in the geological record of the Minusinsk Basin was expressed in their attempts to establish a continuous series of palaeontological and palaeofloral assemblages based on traditional ideas of continuous succession, which led to erroneous taxonomic definitions and incorrect interpretations of biostratigraphic age. New radioisotopic dating confirms Sivtchikov's observations (Sivtchikov and Donova, 2016) and determines the duration of the hiatus between the Izykh and Narylkova Fms to be about 5 Ma.

7. Conclusions

The petrography, structure, and mineralogical composition of the studied tonsteins confirm their origin from volcanic ash-falls. Results from X-ray diffraction analysis (XRD), energy-dispersive X-ray spectrometry (SEM-EDS), and inductively coupled plasma mass spectrometry (ICP-MS) establish the composition of the parent pyroclastic material as rhyolite-pantellerite for tonstein I-22 and more basic, dacite-rhyodacite, for tonstein I-12.

Morphological analysis of zircon crystals, as well as the results of the cathodoluminescence and melt inclusion studies, confirm the unity of the mineral populations extracted from the tonsteins and the crystallisation of zircons from volcanic material at temperatures ranging from 700 to 900ºC.

New radioisotopic dates of 261.4 ± 0.7 Ma and 261.3 ± 0.4 Ma clarify the age of the Izykh Formation, enabling direct correlation of its upper part, including the XXX coal seam, with the Capitanian stage of the International Chronostratigraphic Chart.

The results highlight the discontinuity and incompleteness of the coal-bearing succession of southern Angaraland, where gaps can span several million years.

The data demonstrate the potential for radioisotopic dating of tonsteins, which are abundant in the coal-bearing strata of the Minusinsk Basin. Continuation of such work may provide new insights into the stratigraphic framework of coal seams and clarify the structure and history of Upper Palaeozoic coal accumulation in southern Angaraland.

 doi:10.20944/preprints202407.1814.v1

Author Contributions:

Funding:

Conflicts of Interest:

References

1. Admakin, L.A. Types of tonsteins in coal beds of Minusinsk basin. *Lithol. Min. Res.* **1992**, *2*, 49–56. (In Russian)
2. Annen, C.; Zellmer, G.F. *Dynamics of crustal magma transfer, storage and differentiation*; Geological Society: London, UK, Special Publications, 2008; Volume 304(1), pp. 35–59. https://doi.org/10.1144/SP304
3. Arbuzov, S.I.; Ershov, V.V.; Rikhvanov, L.P.; Kyargin, V.V.; Bulatov, A.A.; Dubovik, P.E. Rare-metal potential of coals of Minusinsk basin; Publishing House SO RAN Branch "GEO": Novosibirsk, Russia, 2003; 347p. (In Russian)
4. Arbuzov, S.I.; Mezhibor, A.M.; Spears, D.A.; Ilenok, S.S.; Shaldybin, M.V.; Belaya, E.V. Nature of tonsteins in the Azeisk deposit of the Irkutsk Coal Basin (Siberia, Russia). *Int. J. Coal Geol.* **2016**, *153*, 99–111. https://doi.org/10.1016/j.coal.2015.12.001
5. Arbuzov, S.I.; Ilenok, S.S.; Vergunov, A.V.; Shaldybin, M.V.; Sobolenko, V.M.; Nekrasov, P.E. Mineralogical-geochemical identification of explosive volcanism products in coals of the Minusinsk basin. In *Petrology of magmatic and metamorphic complexes. Issue 9*, Proceedings of 9th All-Russian petrographic conference; CSTI: Tomsk, Russia, 2017; pp. 35–37. (In Russian).
6. Arbuzov, S.I.; Spears, D.A.; Vergunov, A.V.; Ilenok, S.S.; Mezhibor, A.M.; Ivanov, V.P.; Zarubina, N.A. Geochemistry, mineralogy and genesis of rare metal (Nb-Ta-Zr-Hf-Y-REE-Ga) coals of the seam XI in the south of Kuznetsk Basin, Russia. *Ore Geol. Rev.* **2019**, *113*, 103073. https://doi.org/10.1016/j.oregeorev.2019.103073
7. Benisek, A.; Finger, F. Factors controlling the development of prism faces in granite zircons: a microprobe study. *Contributions to Mineralogy and Petrology* **1993**, *114(4)*, 441–451. https://doi.org/10.1007/bf00321749
8. Betekhtina, O.A.; Gorelova, S.G.; Dryagina, L.L.; Danilov, V.I.; Batyaeva, S.P.; Tokareva, P.A. Upper Paleozoic of Angarida; Zhuravleva, I.T., Ilyina, V.I., Eds.; Nauka: Novosibirsk, Russia, 1988; 265p. (In Russian)
9. Bezzubtsev, V.V.; Perfilova, O.Y. State Geological Map of Russian Federation; Scale 1: 1 000 000. Third generation. Series Altai-Sayan. Sheet N-46 (Abakan); Cartographic factory "VSEGEI": St. Petersburg, 2008; 391p. (In Russian) https://www.geokniga.org/sites/geokniga/files/mapcomments/n-46-abakan-gosudarstvennaya-geologicheskaya-karta-rossiyskoy-federacii-tre.pdf
10. Bish, D.L.; Post, J.E. Quantitative mineralogical analysis using the Rietveld fullpattern fitting method. *Am. Min.* **1993**, *78*, 932–940.
11. Black, L.P.; Kamo, S.L.; Allen, C.M.; Davis, D.W.; Aleinikoff, J.N.; Valley, J.W.; Mundil, R.; Campbell, I.H.; Korsch, R.J.; Williams, I.S.; et al. Improved 206Pb/238U microprobe geochronology by the monitoring of a trace-element related matrix effect; SHRIMP, ID-TIMS, ELA-ICP-MS and oxygen isotope documentation for a series of zircon standards. *Chem. Geol.* **2004**, *205*, 115–140. https://doi.org/10.1016/j.chemgeo.2004.01.003
12. Bohor, B.F.; Triplehorn, D.M. Tonsteins: Altered Volcanic-Ash Layers in Coal-Bearing Sequences. In *Geological Society of America Special Papers*; Boulder, USA, 1993; Volume 285, pp. 1–44. https://doi.org/10.1130/SPE285
13. Bowring, J.F.; McLean, N.M.; Bowring, S.A. Engineering cyber infrastructure for U-Pb geochronology: Tripoli and U-Pb_Redux. *Geochem. Geophys. Geosystems* **2011**, 12, Q0AA19. https://doi.org/10.1029/2010GC003479
14. Budnikov, I.V. (Ed.) Decision of the Meeting on the stratigraphy of the Upper Paleozoic deposits of Kuzbass. *In Kuznetsk Basin—Key Region in Stratigraphy of the Angarida Upper Paleozoic*; YuzhSibgeolkom: Novosibirsk, Russia, 1996; Volume 2, pp. 93–94. (In Russian)
15. Budnikov, I.V.; Kutygin, R.V.; Shi, G.R.; Sivtchikov, V.E.; Krivenko, O.V. Permian stratigraphy and paleogeography of Central Siberia (Angaraland) – A review. *Journal of Asian Earth Sciences* **2020**, *196(February)*, 104365. https://doi.org/10.1016/j.jseaes.2020.104365

16. Burger, K.; Bandelow, F.K.; Bieg, G. Pyroclastic kaolin coal–tonsteins of the Upper Carboniferous of Zonguldak and Amasra. *Turkey. Int. J. Coal Geol.* **2000**, *45*, 39–53. https://doi.org/10.1016/S0166-5162(00)00021-5
17. Cagliari, J.; Schmitz, M.D.; Tedesco, J.; Trentin, F.A.; Lavina, E.L.C. High-precision U-Pb geochronology and Bayesian age-depth modelling of the glacial-postglacial transition of the southern Paraná Basin: Detailing the terminal phase of the Late Paleozoic Ice Age on Gondwana. *Sedimentary Geology* **2023**, *451*, 106397. https://doi.org/10.1016/J.SEDGEO.2023.106397
18. Cagliari, J.; Lavina, E.L.C.; Philipp, R.P.; Tognoli, F.M.W.; Basei, M.A.S.; Faccini, U.F. New Sakmarian ages for the Rio Bonito formation (Paraná Basin, southern Brazil) based on LA-ICP-MS U-Pb radiometric dating of zircons crystals. *Journal of South American Earth Sciences* **2014**, *56*, 265–277. https://doi.org/10.1016/j.jsames.2014.09.013.
19. Cao, W.; Zahirovic, S.; Flament, N.; Williams, S.; Golonka, J.; Müller, R.D. Improving global paleogeography since the late Paleozoic using paleobiology. *Biogeosciences* **2017**, 14, 5425–5439. https://doi.org/10.5194/bg-14-5425-2017
20. Chernovyants, M.G. Tonsteins and Their Use in the Study of Coalbearing Formations; Nedra: Moscow, Russia, 1992; 144p. (In Russian)
21. Ghiorso, M.S.; Sack, R.O. Chemical mass transfer in magmatic processes IV. A revised and internally consistent thermodynamic model for the interpolation and extrapolation of liquid-solid equilibria in magmatic systems at elevated temperatures and pressures. *Contributions to Mineralogy and Petrology* **1995**, *119(2–3)*, 197–212. https://doi.org/10.1007/BF00307281
22. Condon, D.J.; Schoene, B.; McLean, N.M.; Bowring, S.A.; Parrish, R.R. Metrology and traceability of U–Pb isotope dilution geochronology (EARTHTIME Tracer Calibration Part I). *Geochim. Cosmochim. Acta* **2015**, *164*, 464–480. https://doi.org/10.1016/j.gca.2015.05.026
23. Dai, S.; Zhou, Y.; Zhang, M.; Wan, G.X.; Wang, J.; Song, X.; Jiang, Y.; Luo, Y.; Song, Z.; Yang, Z.; Ren, D. A new type of Nb (Ta)-Zr(Hf)-REE-Ga polymetallic deposit in the late Permian coal-bearing strata, eastern Yunnan, southwestern China: Possible economic significance and genetic implications. *Int. J. Coal Geol.* **2010**, *83*, 55–63. https://doi.org/10.1016/j.coal.2010.04.002
24. Dai, S.; Ward, C.R.; Graham, I.T.; French, D.; Hower, J.C.; Zhao, L.; Wang, X. Altered volcanic ashes in coal and coal-bearing sequences: a review of their nature and significance. *Earth-Sci. Rev.* **2017**, *175*, 44–74. https://doi.org/10.1016/j.earscirev.2017.10.005
25. Dai, S.; Nechaev, V.P.; Chekryzhov, I.Y.; Zhao, L.; Vysotskiy, S.V.; Graham, I.; Ward, C.R.; Ignatiev, A.V.; Velivetskaya, T.A.; Zhao, L. A model for Nb–Zr–REE–Ga enrichment in Lopingian altered alkaline volcanic ashes: Key evidence of H-O isotopes. *Lithos* **2018**, *302–303*, 359–369. https://doi.org/10.1016/j.lithos.2018.01.005
26. Davydov V.I.; Crowley J.L.; Schmitz M.D.; Poletaev V.I. High-Precision U-Pb Zircon Age Calibration of the Global Carboniferous Time Scale and Milankovitch Band Cyclicity in the Donets Basin, Eastern Ukraine. *Geochemistry Geophysics Geosystems* **2010**, *11*, Q0AA04. https://doi.org/10.1029/2009gc002736
27. Davydov, V.I.; Korn, D.; Schmitz, M.D. The Carboniferous period. In *The Geologic Time Scale*, 1st ed.; Gradstein, F.M., Ogg, J.G., Schmitz, M., Ogg, G., Eds.; Elsevier: Oxford, UK, 2012; pp. 603–651. https://doi.org/10.1016/B978-0-444-59425-9.00023-8
28. Davydov, V.I.; Arefiev, M.P.; Golubev, V.K.; Karasev, E.V.; Naumcheva, M.A.; Schmitz, M.D.; Silantiev, V.V.; Zharinova, V.V. Radioisotopic and biostratigraphic constraints on the classical Middle–Upper Permian succession and tetrapod fauna of the Moscow syneclise, Russia. *Geology* **2020**, *48*, 742–747. https://doi.org/10.1130/G47172
29. Davydov, V.I.; Karasev, E.V.; Nurgalieva, N.G.; Schmitz, M.D.; Budnikov, I.V.; Biakov, A.S.; Kuzina, D.M.; Silantiev, V.V.; Urazaeva, M.N.; Zharinova, V.V.; Zorina, S.O.; Gareev, B.; Vasilenko, D.V. Climate and biotic evolution during the Permian-Triassic transition in the temperate Northern Hemisphere, Kuznetsk Basin, Siberia, Russia. *Palaeogeography, Palaeoclimatology, Palaeoecology* **2021**, *573(April)*, 110432. https://doi.org/10.1016/j.palaeo.2021.110432
30. *Decisions of the All-Union Conference on the Development of Unified Stratigraphic Schemes for the Precambrian, Paleozoic and Quaternary Systems of Central Siberia (Novosibirsk, 1979). Part 2 (Middle and Upper Paleozoic)*; SRIGGMRM: Novosibirsk, Russia, 1982; 129p. (In Russian)

31. Demchuk, T.D.; Nelson-Glatiotis, D.A. The identification and significance of kaolinite-rich, volcanic ash horizons (tonsteins) in the Ardley coal zone, Wabamun, Alberta, Canada. *Bulletin of Canadian Petroleum Geology* **1993**, *41(4)*, 464–469. https://doi.org/10.35767/gscpgbull.41.4.464
32. Ducassou, C.; Mercuzot, M.; Bourquin, S.; Rossignol, C.; Pellenard, P.; Beccaletto, L.; Poujol, M.; Hallot, E.; Pierson-Wickmann, A.C., Hue, C.; Ravier, E. Sedimentology and U-Pb dating of Carboniferous to Permian continental series of the northern Massif Central (France): Local palaeogeographic evolution and larger scale correlations. *Palaeogeography, Palaeoclimatology, Palaeoecology* **2019**, *533(February)*, 109228. https://doi.org/10.1016/j.palaeo.2019.06.001
33. Dryagina, L.L. Palynological assemblages of coal seams of the Izykh deposit of the Minusinsk basin. In *Coal-bearing sediments of the Kuznetsk and Tunguska provinces*; Zvonarev, I.N., Ed.; SNIIGGiMS: Novosibirsk, USSA, **1975**; pp. 57–58. (Proceedings of the SNIIGGiMS, *221*). (In Russian)
34. Fedotov, A.N.; Ladygin, S.V.; Izmailova, S.A.; Sivtchikov, V.E.; Kalinin, V.V.; Izmaylova, S.A.; Kalinin, V.A.; Tsareva, E.V.; Lysogorsky, K.V.; Kacheev, Yu.F. State Geological map of Russian Federation; Scale 1 : 200 000. Second edition. Minusinsk series. Sheet N-46-XX (Abakan). Explanatory note (Electronic resource); Ministry of Natural Resources of Russia, Rosnedra. Moscow branch of FSBI "VSEGEI": Moscow, Russia, 2019; 78p. (In Russian) https://www.geokniga.org/maps/31048
35. Fedotova, V.A.; Fedotov, A.N. Minusinsk Coal Basin. General information. Geological overview. Coal-bearing capacity. In *Coal Base of Russia. Coal Basins and Deposits of Eastern Siberia*, Cherepovsky, V.F., Ed.; LLC "Geoinformcentre": Moscow, Russia, 2002; Volume 3, pp. 173–201. (In Russian)
36. Feng, Y.; Yang, T.; Liang, F.; Liu, F.; Sun, G. New zircon U–Pb age of the Didao Formation in Jixi Basin and its significance for the geology and paleogeography in Jixi and eastern Heilongjiang region in the Early Cretaceous. *Cretaceous Research* **2022**, *135*, 105169. https://doi.org/10.1016/J.CRETRES.2022.105169
37. Gerstenberger, H.; Haase, G. A highly effective emitter substance for mass spectrometric Pb isotope ratio determinations. *Chem. Geol*. **1997**, *136*, 309–312.
38. Grigoryev, N.A. About chemical elements Clark content in the upper part of continental crust. *Litosphera (Lithosphere)* **2002**, *1*, 61–71. (In Russian)
39. Grigorev, N.A. Average concentrations of chemical elements in rocks of the upper continental crust. *Geochemistry International* **2003**, *41(7)*, 711–718.
40. Gorelova, S.G. Phytostratigraphic characterisation of coal-bearing sediments of the Minusinsk basin. In *Coal-bearing sediments of the Kuznetsk and Tunguska provinces*; Zvonarev, I.N., Ed.; SNIIGGiMS: Novosibirsk, Russia, **1975**; pp. 47–56. (Proceedings of the SNIIGGiMS, *221*). (In Russian)
41. Gorelova, S.G.; Budnikov, I.V. Main stages of studying the stratigraphy of the Upper Palaeozoic of Kuzbass. In *Kuznetsk Basin – key region in stratigraphy of the Angarida Upper Paleozoic*; Budnikov, I.V., Ed.; YuzhSibgeolkom: Novosibirsk, Russia, 1996; Volume 1, pp. 7–12. (In Russian)
42. Gromet, L.P.; Haskin, L.A.; Korotev, R.L.; Dymek, R.F. The "North American shale composite": Its compilation, major and trace element characteristics. Geo*chim. Cosmochim. Acta* **1984**, *48*, 2469–2482. https://doi.org/10.1016/0016-7037(84)90298-9
43. Guerra-Sommer, M.; Cazzulo-Klepzig, M.; Santos, J.O.S.; Hartmann, L.A.; Ketzer, J.M.; Formoso, M.L.L. Radiometric age determination of tonsteins and stratigraphic constraints for the Lower Permian coal succession in southern Paraná Basin, Brazil. *International Journal of Coal Geology* **2008**, *74(1)*, 13–27. https://doi.org/10.1016/j.coal.2007.09.005
44. Hower, J.C.; Rupport, L.F.; Cortland, F.E. Lanthanide, yttrium, and zirconium anomalies in the Fire Clay coal bed, Eastern Kentucky. *Int. J. Coal Geology* **1999**, *39(1–3)*, 141–153.
45. International Chronostratigraphic Chart. Available online: https://stratigraphy.org/ICSchart/ChronostratChart2023-06.pdf (accessed on 07 July 2024).
46. Jirásek, J.; Opluštil, S.; Sivek, M.; Schmitz, M.D.; Abels, H.A. Astronomical forcing of Carboniferous paralic sedimentary cycles in the Upper Silesian Basin, Czech Republic (Serpukhovian, latest Mississippian): New radiometric ages afford an astronomical age model for European biozonations and substages. *Earth-Science Reviews* **2018**, *177*, 715–741. https://doi.org/10.1016/J.EARSCIREV.2017.12.005
47. Jurigan, I.; Ricardi-Branco, F.; Neregato, R.; dos Santos, T.J.S. A new tonstein occurrence in the eastern Paraná Basin associated with the Figueira coalfield (Paraná, Brazil): Palynostratigraphy and U-Pb radiometric dating integration. *Journal of South American Earth Sciences* **2019**, *96(August)*, 102377. https://doi.org/10.1016/j.jsames.2019.102377

48. Käßner, A.; Tichomirowa, M.; Lapp, M.; Leonhardt, D.; Whitehouse, M.; Gerdes, A. Two-phase late Paleozoic magmatism (~313–312 and ~299–298 Ma) in the Lusatian Block and its relation to large scale NW striking fault zones: Evidence from zircon U–Pb CA–ID–TIMS geochronology, bulk rock- and zircon chemistry. *Int. J. Earth Sci.* **2021**, *110*, 2923–2953. https://doi.org/10.1007/s00531-021-02092-y
49. Ketris, M.P.; Yudovich, Y.E. Estimations of Clarkes for Carbonaceous biolithes: World averages for trace element contents in black shales and coals. *International Journal of Coal Geology* **2009**, *78(2)*, 135–148. https://doi.org/10.1016/j.coal.2009.01.002
50. Loughnan, F.C. Flint clays, tonsteins and the kaolinite clayrock facies. *Clay Minerals* **1978**, *13(4)*, 387–400. https://doi.org/10.1180/claymin.1978.013.4.04
51. Lyons, P.C.; Krogh, T.E.; Kwok, Y.Y.; Davis, D.W.; Outerbridge, W.F.; Evans, H.T. Radiometric ages of the Fire Clay tonstein (Pennsylvanian (Upper Carboniferous), Westphalian, Duckmantian): A comparison of U-Pb zircon single-crystal ages and 40Ar/39Ar sanidine single-crystal plateau ages. *International Journal of Coal Geology* **2006**, *67(4)*, 259–266. https://doi.org/10.1016/j.coal.2005.12.002
52. Lyons, P.C.; Spears, D.A.; Outerbridge, W.F.; Congdon, R.D.; Evans, H.T. Euramerican tonsteins: overview, magmatic origin, and depositional-tectonic implications. *Palaeogeography, Palaeoclimatology, Palaeoecology* **1994**, *106(1–4)*, 113–134. https://doi.org/10.1016/0031-0182(94)90006-X
53. Markl, G. *Minerale und Gesteine*. *Mieneralogie – Petrologie – Geochemie*, 2. Auflage; Spectrum Akademischer Verlag: Heidelberg, Germany, 2008; 61p. (In German)
54. Mattinson, J.M. Zircon U-Pb chemical abrasion ("CA-TIMS") method: Combined annealing and multi-step partial dissolution analysis for improved precision and accuracy of zircon ages. *Chem. Geol.* **2005**, *220*, 47–66. https://doi.org/10.1016/j.chemgeo.2005.03.011
55. Metcalfe, I.; Crowley, J.L.; Nicoll, R.S.; Schmitz, M. High-precision U-Pb CA-TIMS calibration of Middle Permian to Lower Triassic sequences, mass extinction and extreme climate-change in eastern Australian Gondwana. *Gondwana Research* **2015**, *28(1)*, 61–81. https://doi.org/10.1016/j.gr.2014.09.002
56. Mikheeva, E.A.; Demonterova, E.I.; Khubanov, V.B.; Ivanov, A.V.; Arzhannikova, A.V.; Arzhannikov, S.G.; Blinov, A.V. Age of the coal accumulation in the irkutsk basin based on accessory zircon dating in the azeisk deposit tonstein (LA-ICP-MS). *Vestnik of Saint Petersburg University. Earth Sciences* **2020**, *65(3)*, 420–433. https://doi.org/10.21638/SPBU07.2020.301
57. Moore, D.M.; Reynoldsl Jr., R.C. X-ray Diffraction and the Identification and Analysis of Clay Minerals. Oxford University Press: Oxford, UK, 1997; 400p.
58. Mori, A.L.O.; de Souza, P.A.; Marques, J.C.; Lopes, R. da C. A new U-Pb zircon age dating and palynological data from a Lower Permian section of the southernmost Paraná Basin, Brazil: Biochronostratigraphical and geochronological implications for Gondwanan correlations. *Gondwana Research* **2012**, *21(2–3)*, 654–669. https://doi.org/10.1016/j.gr.2011.05.019
59. Neiburg, M.F. Stratigraphic comparison of coal-bearing sediments of the Minusinsk and Kuznetsk basins in Siberia. In *Proceedings devoted to Academician V.I. Obruchev*; Publishing House of the USSR Academy of Sciences: Moscow, USSA, 1938; Volume 1, pp. 27–40. (In Russian)
60. Opluštil, S.; Laurin, J.; Hýlová, L.; Jirásek, J.; Schmitz, M.; Sivek, M. Coal-bearing fluvial cycles of the late Paleozoic tropics; astronomical control on sediment supply constrained by high-precision radioisotopic ages, Upper Silesian Basin. *Earth-Science Reviews* **2022**, *228*, 103998. https://doi.org/10.1016/J.EARSCIREV.2022.103998
61. Opluštil, S.; Schmitz, M.; Cleal, C.J.; Martínek, K. A review of the Middle–Late Pennsylvanian west European regional substages and floral biozones, and their correlation to the Geological Time Scale based on new U–Pb ages. *Earth-Science Reviews* **2016**, *154*, 301–335. https://doi.org/10.1016/J.EARSCIREV.2016.01.004
62. Pellenard, P.; Gand, G.; Schmitz, M.; Galtier, J.; Broutin, J.; Stéyer, J.S. High-precision U-Pb zircon ages for explosive volcanism calibrating the NW European continental Autunian stratotype. *Gondwana Research* **2017**, *51*, 118–136. https://doi.org/10.1016/j.gr.2017.07.014
63. Pupin, J.P. Zircon and granite petrology. *Contributions to Mineralogy and Petrology* **1980**, *73(3)*, 207–220. https://doi.org/10.1007/BF00381441
64. Radchenko, G.P. Guiding forms of the Upper Paleozoic flora of the Altai-Sayan region. In *Atlas of guiding forms of fossil flora and fauna of Western Siberia*, Part II; Khalfin, L.L., Ed.; Gosgeoltekhizdat: Moscow, USSA, 1955; pp. 42–154. (In Russian)

65. Rudnick, R.L.; Gao, S. Composition of the continental crust. In *Treatise on Geochemistry*; Holland, H.D., Turekian, K.K., Eds.; Elsevier: Amsterdam, 2014; Volume 3, pp. 1–64. https://doi.org/10.1016/B0-08-043751-6/03016-4
66. Schmitz, M.D.; Singer, B.S.; Rooney, A.D. Radioisotope Geochronology. In *Geologic Time Scale 2020*; Gradstein, F.M., Ogg, J.G., Schmitz, M.D., Ogg, G.M.; Elsevier, 2020; Volume 1; pp. 193–209. https://doi.org/10.1016/B978-0-12-824360-2.00006-1
67. Schneider, J.W.; Lucas, S.G.; Scholze, F.; Voigt, S.; Marchetti, L.; Klein, H.; Opluštil, S.; Werneburg, R.; Golubev, V.K.; Barrick, J.E.; Nemyrovska, T.; Ronchi, A.; Day, M.O.; Silantiev, V.V.; Rößler, R.; Saber, H.; Linnemann, U.; Zharinova, V.; Shen, S.-Z. Late Paleozoic–early Mesozoic continental biostratigraphy – Links to the Standard Global Chronostratigraphic Scale. *Palaeoworld* **2020**, *29(2)*, 186–238. https://doi.org/10.1016/j.palwor.2019.09.001
68. Schoene, B.; Crowley, J.L.; Condon, D.C.; Schmitz, M.D.; Bowring, S.A. Reassessing the uranium decay constants for geochronology using ID-TIMS U–Pb data. *Geochim. Cosmochim. Acta* **2006**, *70*, 426–445. https://doi.org/10.1016/j.gca.2005.09.007
69. Shen, M.; Dai, S.; Graham, I.T.; Nechaev, V.P.; French, D.; Zhao, F.; Shao, L.; Liu, S.; Zuo, J.; Zhao, J.; Chen, K.; Xie, X. Mineralogical and geochemical characteristics of altered volcanic ashes (tonsteins and K-bentonites) from the latest Permian coal-bearing strata of western Guizhou Province, southwestern China. *International Journal of Coal Geology* **2021**, *237*, 103707. https://doi.org/10.1016/J.COAL.2021.103707
70. Shen, M.; Dai, S.; Nechaev, V.P.; French, D.; Graham, I.T.; Liu, S.; Chekryzhov, I. Yu.; Tarasenko, I.A.; Zhang, S. Provenance changes for mineral matter in the latest Permian coals from western Guizhou, southwestern China, relative to tectonic and volcanic activity in the Emeishan Large Igneous Province and Paleo-Tethys region. *Gondwana Research* **2023**, *113*, 71–88. https://doi.org/10.1016/j.gr.2022.10.011
71. Shi, G.R.; Nutman, A.P.; Lee, S.; Jones, B.G.; Bann, G.R. Reassessing the chronostratigraphy and tempo of climate change in the Lower-Middle Permian of the southern Sydney Basin, Australia: Integrating evidence from U–Pb zircon geochronology and biostratigraphy. *Lithos* **2022**, *410–411*, 106570. https://doi.org/10.1016/J.LITHOS.2021.106570
72. Silantiev, V.V.; Gutak, Y.M.; Tichomirowa, M.; Kulikova, A.V.; Felker, A.S.; Urazaeva, M.N.; Porokhovnichenko, L.G.; Karasev, E.V.; Bakaev, A.S.; Zharinova, V.V.; et al. First radiometric dating of tonsteins from coal-bearing succession of the Kuznetsk Basin: U-Pb geochronology of the Tailugan Formation. *Georesursy=Georesources* **2023**, *25*, 203–227. https://doi.org/10.18599/grs.2023.2.15
73. Silantiev, V.V.; Gutak, Y.M.; Tichomirowa, M.; Käßner, A.; Kutygin, R.V.; Porokhovnichenko, L.G.; Karasev, E.V.; Felker, A.S.; Bakaev, A.S.; Naumcheva, M.A.; Urazaeva, M.N.; Zharinova, V.V. U-Pb Dating of the Kolchugino Group Basement (Kuznetsk Coal Basin, Siberia): Was the Change in Early–Middle Permian Floras Simultaneous at Different Latitudes in Angaraland? *Geosciences (Switzerland)* **2024**, *14(1)*, 21. https://doi.org/10.3390/geosciences14010021
74. Simas, M.W.; Guerra-Sommer, M.; Cazzulo-Klepzig, M.; Menegat, R.; Schneider Santos, J.O.; Fonseca Ferreira, J.A.; Degani-Schmidt, I. Geochronological correlation of the main coal interval in Brazilian Lower Permian: Radiometric dating of tonstein and calibration of biostratigraphic framework. *Journal of South American Earth Sciences* **2012**, *39*, 1–15. https://doi.org/10.1016/j.jsames.2012.06.001
75. Sivtchikov, V.E.; Donova, N.B. Stratigraphic subdivision of the Upper Palaeozoic deposits of the South Minusinsk Depression. *Lethaea Rossica. Russian Palaeobotanical Journal* **2016**, *13*, 1–46.
76. Sobczak, K.; Cooling, J.; Crossingham, T.; Holl, H.G.; Reilly, M.; Esterle, J.; Crowley, J.L.; Hannaford, C.; Mohr, M.T.; Hamerli, Z.; Hurter, S. Palynostratigraphy and Bayesian age stratigraphic model of new CA-ID-TIMS zircon ages from the Walloon Coal Measures, Surat Basin, Australia. *Gondwana Research* **2024**, *132*, 150–167. https://doi.org/10.1016/J.GR.2024.04.012
77. Spasskaya, I.S. On the assemblages of bivalve molluscs of coal-bearing sediments of the Izykh field in the Minusinsk coal basin. In *Continental Upper Paleozoic and Mesozoic of Siberia and Central Kazakhstan: Biostratigraphy and Palaeontology*; Nalivkin, D.V., Ed.; Nauka: Moscow-Leningrad, USSA, 1966; pp. 5–40. (In Russian)
78. Spears, D.A. A kaolinite mudstone (tonstein) in the British Coal Measures. *J. Sedim. Petrol.* **1970**, *40(1)*, 386–394.
79. Spears, D.A. The origin of tonsteins, an overview, and links with seatearths, fireclays and fragmental clay rocks. *International Journal of Coal Geology* **2012**, *94*, 22–31. https://doi.org/10.1016/J.COAL.2011.09.008

80. Spears, D.A.; Kanaris-Sotiriou, R. A geochemical and mineralogical investigation of some British and other European tonsteins. *Sedimentology* **1979**, *26*, 407–425. https://doi.org/10.1111/j.1365-3091.1979.tb00917.x
81. Spears, D.A.; Arbuzov, S.I. A geochemical and mineralogical update on two major tonsteins in the UK Carboniferous Coal Measures. *International Journal of Coal Geology* **2019**, *210(April)*, 103199. https://doi.org/10.1016/j.coal.2019.05.006
82. *Stratigraphic Guide of Russia*, 3rd ed.; Corrected and supplemented; VSEGEI: St. Petersburg, Russia, 2019; 96p. (In Russian)
83. Taylor, J.C. Computer programs for standardless quantitative analysis of minerals using the full powder diffraction profile. *Powder Diffract*. **1991**, *6*, 2–9. https://doi.org/10.1017/S0885715600016778
84. Taylor, S.R.; McLennan, S.M. *The Continental Crust: Its Composition and Evolution*; Blackwell Scientific Publications: Oxford, UK, 1985; 312p. https://doi.org/10.1002/gj.3350210116
85. Troshkova, G.N.; Zhichko, L.A. Coal-bearing sediments of the Minusinsk basin. In *Stratigraphy of the Palaeozoic of Middle Siberia*; Sokolov B.S., Ed.; Nauka: Novosibirsk, USSA, 1967; pp. 186–189. (In Russian)
86. Vergunov, A.V.; Arbuzov, S.I.; Sobolenko, V.M. Mineralogy and geochemistry of the tonsteins in the coals of the Beisk deposit of Minusinsk Basin. Bull. Tomsk Polytech. *Univ. Geo Assets Eng*. **2019**, *330(2)*, 155–166. (In Russian with English Abstract). https://doi.org/10.18799/24131830/2019/2/116
87. Vergunov, A.V.; Arbuzov, S.I.; Eremeyeva, V.V. Mineralogy, geochemistry and genesis of rare-metal Zr-Nb-Hf-Ta-REE-Ga mineralization in bed XXX of Minusinsk Basin. *Bull. Tomsk Polytech. Univ. Geo Assets Eng.* **2020**, *331(7)*, 49–62. (In Russian with English Abstract). https://doi.org/10.18799/24131830/2020/7/2718
88. Vergunov, A.V.; Arbuzov, S.I.; Spears, D.A.; Kholodov, A.S.; Ilenok, S.S. Mineralogy and geochemistry of rare metal (Zr-Nb-Hf-Ta-REE-Ga) coals of the seam XXX of the Izykh Coalfield, Minusinsk Basin, Russia: Implications for more widespread rare metal mineralization in North Asia. *International Journal of Coal Geology* **2024**, *289*, 104542. https://doi.org/10.1016/j.coal.2024.104542
89. Wang, J.; Shao, L.Y.; Wang, H.; Spiro, B.; Large, D. SHRIMP zircon U–Pb ages from coal beds across the Permian–Triassic boundary, eastern Yunnan, southwestern China. *Journal of Palaeogeography* **2018**, *7(2)*, 117–129. https://doi.org/10.1016/j.jop.2018.01.002
90. Wang, T.; Ramezani, J.; Yang, C.; Yang, J.; Wu, Q.; Zhang, Z.; Lv, D.; Wang, C. High-resolution geochronology of sedimentary strata by U-Pb CA-ID-TIMS zircon geochronology: A review. *Earth-Science Reviews* **2023**, *245*, 104550. https://doi.org/10.1016/J.EARSCIREV.2023.104550
91. Wiedenbeck, M.; Alle, P.; Corfu, F.; Griffin,W.L.; Meier, M.; Oberli, F.; Von Quadt, A.; Roddick, J.C.; Spiegel,W. Three Natural Zircon Standards for U-TH-PB, LU-HF, Trace Element and Ree Analyses. *Geostand. Newsl.* **1995**, *19*, 1–23. https://doi.org/10.1111/j.1751-908X.1995.tb00147.x
92. Yarkov, V.O. About the methods of stratigraphic division of the coal-bearing strata of Kuzbass. In *Kuznetsk Basin – key region in stratigraphy of the Angarida Upper Paleozoic*; Budnikov, I.V., Ed.; YuzhSibgeolkom: Novosibirsk, Russia, 1996; Volume 2, pp. 3–5. (In Russian)
93. Yudovich, Ya.E.; Ketris, M.P. Fundamentals of Lithochemistry; Nauka: St. Petersburg, Russia, 2000; 479p. (In Russian)
94. Zaritsky, P.V. Origin of tonsteins within Donbass coal seams. *Report of the USSR Academy of Sciences* **1967**, *177(2)*, 422–425.
95. Zaritsky, P.V. A review of the study of tonsteins in the Donetz basin. In *Congres International de Stratigraphie et Geologie du Carbonifere, 10th, Madrid, 1983, Comptes Rendus*, Madrid, Spain, 1985; Volume 4, pp. 235–241.
96. Zhang, Z.; Lv, D.; Hower, J.C.; Wang, L.; Shen, Y.; Zhang, A.; Xu, J.; Gao, J. Geochronology, mineralogy, and geochemistry of tonsteins from the Pennsylvanian Taiyuan Formation of the Jungar Coalfield, Ordos Basin, North China. *International Journal of Coal Geology* **2023**, *267*, 104183. https://doi.org/10.1016/J.COAL.2023.104183